Heliyon 10 (2024) e36104

Contents lists available at ScienceDirect

Heliyon

journal homepage: www.cell.com/heliyon

Research article

# Study on the mechanisms and Pharmacodynamic substances of Lian-Gui-Ning-Xin-Tang on Arrhythmia Therapy based on Pharmacodynamic–Pharmacokinetic associations

Liang Jiayu [a,1], Li Xiaofeng [b,*,1], Chen Jinhong [c], Deng Fangjun [d], Fan Boya [e], Zhen Xin [f], Cong Zidong [b], Tao Rui [g], Yu Lu [f], Qian Shule [f], Wang Runying [f], Du Wuxun [b,**]

[a] Department of TCM, The First Affiliated Hospital, Zhejiang University School of Medicine, Zhejiang Hangzhou 310003, China
[b] Department of Cardiology, The Second Affiliated Hospital of Tianjin University of TCM, Tianjin 300150, China
[c] School of Rehabilitation Medicine, Shandong Second Medical University, Shandong Weifang, 261053, China
[d] Department of Cardiology, Tianjin Academy of Traditional Chinese Medicine Affiliated Hospital, Tianjin 300091, China
[e] Department of Medical qualification examination, National Administration of Traditional Chinese Medicine TCM Qualification Certification Center, Beijing 100120, China
[f] Graduate School, Tianjin University of TCM, Tianjin 301617, China
[g] Department of TCM, Tianjin University of TCM, Tianjin, 301617, China

ARTICLE INFO

*Keywords:*
Lian-Gui-Ning-Xin-Tang
Arrhythmias
Pharmacodynamic substances
Mechanism
Pharmacodynamics
Pharmacokinetics

ABSTRACT

*Background:* The Chinese herbal compound Lian-Gui-Ning-Xin-Tang (LGNXT), composed of 9 herbs, has a significant antiarrhythmic effect. Previous studies have confirmed that preventing intracellular $Ca^{2+}$ overload and maintaining intracellular $Ca^{2+}$ homeostasis may be the important antiarrhythmic mechanisms of LGNXT. Recent studies are focused on elucidating the mechanisms and pharmacodynamic substances of LGNXT.

*Purpose:* 1) To investigate the antiarrhythmic mechanisms of LGNXT; 2) to explore the association of pharmacodynamics (PD) and pharmacokinetics (PK) of the potential pharmacodynamic substances in LGNXT to further verify the mechanisms of action.

*Methods:* First, pharmacodynamic studies were conducted to determine the effect of LGNXT in arrhythmia at the electrophysiological, molecular, and tissue levels, and the "effect–time" relationship of LGNXT was further proposed. Next, an HPLC-MS/MS method was established to

*Abbreviations:* AC, adenylyl cyclase; Adr, adrenaline; ATP, adenosine triphosphate; AUC, area under the curve; $AUC_{0-24\ h}$, area under the curve from time 0–24 h; $AUC_{0-\infty}$, area under the curve from time 0–infinity; β-AR, β-adrenergic receptor; cAMP, cyclic adenosine monophosphate; CE, collision energy; Cmax, peak concentration; CaM, calmodulin; CaMKII, calcium/calmodulin-dependent protein kinase II; CP, plasma concentration; Cx43, connexin43; DP, declustering potential; EC, effect-site concentration; ECG, electrocardiogram; Emax, maximum effect; GAPDH, glyceraldehyde-3-phosphate dehydrogenase; Gs, stimulatory G protein; IL-6, interleukin-6; LGNXT, Lian-Gui-Ning-Xin-Tang; LLOQ, lower limit of quantification; LPO, lipid hydroperoxide; LTCC, L-type $Ca^{2+}$ channel current; MDA, malondialdehyde; MF, matrix effect; MIT, mitochondria; NKA, $Na^{+}$-$K^{+}$-ATPase; PD, pharmacodynamics; PK, pharmacokinetics; PKA, protein kinase A; RE, relative error; SD, Sprague-Dawley; $t_{1/2}$, elimination half-life; SERCA, $Ca^{2+}$-ATPase; SOD, superoxide dismutase; SR, sarcoplasmic reticulum; TCM, traditional Chinese medicine; Tmax, time to achieve Cmax; WB, Western blot.

* Corresponding author.
** Corresponding author.
*E-mail addresses:* 624129221@qq.com (L. Xiaofeng), cnduwux@163.com (D. Wuxun).
[1] These authors contributed equally to this work.

https://doi.org/10.1016/j.heliyon.2024.e36104
Received 24 October 2023; Received in revised form 8 August 2024; Accepted 9 August 2024
Available online 14 August 2024

identify the "dose–time" relationship of the 9 potential compounds. Combining the "effect–time" and "dose–time" curves, the active ingredients closely related to the inhibition of inflammation, oxidative stress, and energy metabolism were identified to further verify the mechanisms and pharmacodynamic substances of LGNXT.

*Results:* Pretreatment with LGNXT could delay the occurrence of arrhythmias and reduce their duration and severity. LGNXT exerted antiarrhythmic effects by inhibiting MDA, LPO, IL-6, and cAMP; restoring Cx43 coupling function; and upregulating SOD, $Ca^{2+}$-ATPase, and $Na^{+}$-$K^{+}$-ATPase levels. PK-PD association showed that nobiletin, methylophiopogonanone A, trigonelline, cinnamic acid, liquiritin, dehydropolisic acid, berberine, and puerarin were the main pharmacodynamic substances responsible for inhibiting the inflammatory response in arrhythmia. Methylophiopogonanone A, dehydropalingic acid, nobiletin, trigonelline, berberine, and puerarin in LGNXT exerted antiarrhythmic effects by inhibiting oxidative stress. Dehydropalingic acid, berberine, cinnamic acid, liquiritin, puerarin, trigonelline, methylophiopogonanone A, nobiletin, and tetrahydropalmatine exerted antiarrhythmic effects by inhibiting the energy-metabolism process.

*Conclusions:* LGNXT had a positive intervention effect on arrhythmias, especially ventricular tachyarrhythmias, which could inhibit inflammation, oxidative stress, and energy metabolism; positively stabilize the structure, and remodify the function of myocardial cell membranes. Additionally, the PD–PK association study revealed that methylophiopogonanone A, berberine, trigonelline, liquiritin, puerarin, tetrahydropalmatine, nobiletin, dehydropachymic acid, and cinnamic acid directly targeted inflammation, oxidative stress, and energy metabolism, which could be considered the pharmacodynamic substances of LGNXT. Thus, the antiarrhythmic mechanisms of LGNXT were further elucidated.

## 1. Introduction

Arrhythmias are among the major cause of morbidity and mortality worldwide, and there has been a steady increase in the number of patients diagnosed with this condition. The onset of cardiac arrhythmias depends on the electrophysiological and structural properties of cardiac tissue [1], including abnormal or enhanced impulse generation (i.e., focal activity) and conduction disturbances (i.e., reentry) [2,3]. Although numerous approved antiarrhythmic drugs are available, most lack specificity and have the potential to aggravate preexisting arrhythmias or provoke new episodes. Moreover, the mechanisms and comparative effectiveness of drugs used clinically to treat arrhythmias are not well elucidated, which underscores the need for novel agents that can act rapidly and/or more effectively.

As the treatment of arrhythmias is becoming increasingly diverse, traditional Chinese medicine (TCM) has been reported to be efficacious in relieving clinical symptoms, adjusting heart rhythm, controlling the two-way heart rate, and improving the quality of life of patients [4]. The mechanisms involve the comprehensive regulation characteristics and advantages of multicomponent, multipathway, and multitarget effects, which coincide with the ideal principle to treat arrhythmias. LGNXT is a specific formula for the treatment of arrhythmias [5–7]. This formula is based on the Jiaotai pill that is composed of 9 herbs including *Coptis chinensis* Franch. 15g, *Ophiopogon japonicus* Thunb. Ker-Gawl. 12g, *Kudzu vine* root 15g, *Citrus reticulata* Blanco. 10g, *Pinellia ternate* Thunb. Makino 9g, *Poria cocos* Schw. Wolf. 15g, *Cinnamomum cassia* Presl. 3g, *Corydalis acropteryx* Fedde. 12g, and *Glycyrrhiza uralensis* Fisch. 10g, according to Chinese Pharmacopoeia. In previous studies [5], the compounds believed to be responsible for the overall antiarrhythmic effect of LGNXT were obtained based on *in vivo* and *in vitro* studies. Using a systematic pharmacology strategy and *in vivo* pharmacological validation, we clarified the clinical efficacy of LGNXT and proposed that one of its antiarrhythmic mechanisms was attributed to preventing intracellular $Ca^{2+}$ overload and maintaining intracellular $Ca^{2+}$ homeostasis. However, as a TCM compound containing thousands of components, the comprehensive and systematic elucidation of the antiarrhythmic mechanism of LGNXT is crucial. Therefore, in this study, we further investigated the pharmacological mechanism of LGNXT and identified its pharmacodynamic substances.

Arrhythmias were induced in rats by a tail vein injection of adrenaline (Adr). A systems pharmacology approach was used to explore the pharmacodynamic mechanism of LGNXT in treating arrhythmic manifestations such as inflammation, oxidative stress, and energy metabolism, and the "effect–time" relationship was analyzed. An HPLC-MS/MS method was established to identify the "dose–time" relationship of the 9 potential pharmacodynamic substances, including berberine, trigonelline, liquiritin, puerarin, methylophiopogonanone A, tetrahydropalmatine, dehydropachymic acid, nobiletin, and cinnamic acid. After combining the "effect–time" and "dose–time" curves, PK and PD were included to describe the overall relationship of the "dose–time effect", and to identify the pharmacological target of each active ingredient responsible for the antiarrhythmic mechanism of LGNXT, verify the pharmacodynamic substances. Thus, this study adds further value to previous basic reports of LGNXT that use the TCM research mode, reveals the scientific connotation of LGNXT as an antiarrhythmic agent, and provides a basis for the treatment of arrhythmias with TCM.

## 2. Materials and methods

### 2.1. Reagents and materials

A Medlab RU/4C50R multichannel physiological signal acquisition and processing system was purchased from Shanghai Tongyu Teaching Instrument Manufacturing Co., Ltd (Shanghai, China, batch no.17,060,155). Liquid phase meter (Acquity TM UPLC) and mass spectrometer (Synapt TM High-Definition MS [HDMS] System) were purchased from Waters Corporation (Milford, Ma, USA). LGNXT pieces consisted of *Coptis chinensis* Franch. (18122710), *Ophiopogon japonicus* Thunb. Ker-Gawl. (20040803), *Kudzu vine* root (20072002), *Citrus reticulata* Blanco. (19062703), *Pinellia ternate* Thunb. Makino (20190907), *Poria cocos* Schw. Wolf. (20190707), *Cinnamomum cassia* Presl. (20052401), *Corydalis acropteryx* Fedde. (200601), and *Glycyrrhiza uralensis* Fisch. (19091516), were purchased from the pharmacy of the Second Affiliated Hospital of Tianjin University of Traditional Chinese Medicine, Tianjin, China. The voucher specimens were deposited in the Second Affiliated Hospital of Tianjin University of Traditional Chinese Medicine, Tianjin, China. Adr hydrochloride injection was purchased from Tianjin Jinyao Pharmaceutical Co., Ltd. (Tianjin, China, batch no. H12020526). Metoprolol tartrate was purchased from AstraZeneca Pharmaceutical Co., Ltd. (London, England, batch no. H32025391). Cyclic adenosine monophosphate (cAMP), interleukin-6 (IL-6), lipid hydroperoxide (LPO), malondialdehyde (MDA), superoxide dismutase (SOD), $Ca^{2+}$-ATPase (SERCA), and $Na^{+}$-$K^{+}$-ATPase (NKA) (202,101) enzyme-linked immunosorbent assay (ELISA) kits were sourced from Tianjin Zihan Biotechnology (Tianjin, China). Connexin43 (Cx43) (ab11370) and glyceraldehyde-3-phosphate dehydrogenase (GAPDH) (AB-P-R 001) were sourced from Abcam and Hangzhou Xianzhi Biological Co., Ltd., respectively. The reference standards, berberine (D1225AS) and puerarin (N1115AS) were purchased from Dalian Meilun Biotechnology Co., Ltd. (Dalian, China). Trigonelline (A03GB156839) was purchased from Shanghai Yuanye Bio-Technology Co., Ltd. (Shanghai, China). Liquiritin (K2004094) was purchased from Shanghai Aladdin Biochemical Technology Co., Ltd. (Shanghai, China). Cinnamic acid (DST200614-063), tetrahydropalmatine (DSTDY010101), dehydropachymic acid (DSTDQ010101), and methylophiopogonanone A (DST211120-022) were purchased from Chengdu Lemeitian Pharmaceutical Technology Co., Ltd. (Chengdu, China). Nobiletin (MUST-20041210) and naringin (MUST-20041803) were purchased from Baoji Chenguang Biotechnology Co., Ltd. (Baoji, China). Methanol (154,449) and acetonitrile (071,757) were purchased from Fisher Scientific International Inc. (Fair Lawn, NJ). Formic acid was purchased from CNW Technologies GmbH (Duesseldorf, NRW, Germany, batch no. 3208K240). Water was prepared using a Milli-Q water purification system (Millipore, Bedford, MA, USA).

#### 2.1.1. Animal grouping and model establishment

Sterile-pathogen-free (SPF)–grade male Sprague Dawley (SD) rats weighing 230 ± 20 g were purchased from the Animal Experiment Center of the Institute of Health and Medical Sciences, PLA [license no. SCXK (Beijing) 2019-0002]. All experimental animals were housed in an SPF animal laboratory of the experimental animal center of the Institute of Radiation Medicine Chinese Academy of Medical Sciences at an ambient temperature of 23 ± 2 °C and humidity of 35 ± 5 %. All animal experiments were approved by the Animal Care Committee of the Institute of Radiation Medicine, Chinese Academy of Medical Sciences and performed in accordance with the relevant guidelines and regulations.

Rats (n = 72) were acclimatized to the environment for 1 week and provided free access to a standard pellet diet before initiating experiments. The rats were randomly divided into the following six groups with eight rats per group: Control group, Model group, high-dose LGNXT–treated (LGNX-20.77 g/kg/d) group, medium-dose LGNXT–treated (LGNX-10.39 g/kg/d) group, low-dose LGNXT–treated (LGNX-5.19 g/kg/d) group, and metoprolol tartrate (Meto) group. The Meto group received 2.57 g/kg/d metoprolol tartrate, whereas the Control and Model groups were administered an equal volume of 0.9 % normal saline (5 mL/kg/d). Intragastric administration was performed once daily for 14 consecutive days. LGNXT dosage was converted based on the clinical dosage, and the medium dose was equivalent to the clinical dose used routinely.

### 2.2. Determination of the therapeutic mechanism LGNXT in arrhythmias

(1) Electrocardiography

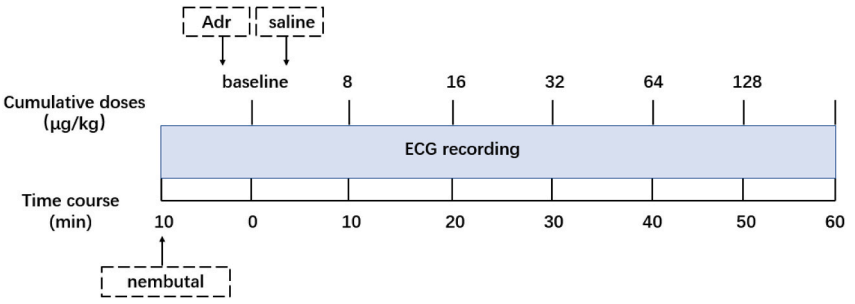


**Fig. 1.** Adr-induced arrhythmias in rats anesthetized using pentobarbital. Adr: adrenaline; Saline: 0.9 % normal saline. Rats were anesthetized and their electrocardiograms were recorded for at least 10 consecutive minutes to ensure normal readings prior to modeling.

Rats were intraperitoneally anesthetized with 0.6 % nembutal (30 mg/kg) 30 min after the last administration of LGNXT. They were then fixed on a plank in a prone position with the limbs subcutaneously connected to the Medlab® RU/4C50R biological information-acquisition system. A standard lead II electrocardiogram was obtained (paper speed 50 mm/s) for stabilization and the baseline was adjusted to zero. Rats were subsequently injected with Adr via the tail vein after stabilization of the electrocardiogram (ECG) to establish the arrhythmia model.

Based on the method reported by Hashimoto [8], arrhythmia was induced by cumulative bolus doses of Adr (8, 16, 32, 64, and 128 mg/kg) given at 10-min intervals or until their death (Fig. 1). Rats in the Control group were injected an equal volume of 0.9 % normal saline. The onset and duration of arrhythmia were analyzed using Lambeth conventions [9], and the QRS duration and QTc interval were determined using Bazzett's formula $QTc = QT/\sqrt{RR}$ [10].

All rats were euthanized after ECG acquisition; 1.5 mL of venous blood was immediately collected from the retro-ocular venous plexus and the hearts were isolated. Blood was centrifuged at 3000×*g* at 4 °C for 10 min, and appropriate amount of myocardial tissue was ground, centrifuged at 13000×*g* at 4 °C for 10min. All samples were stored at −80 °C until ELISAs and western blotting (WB) were performed.

(2) ELISA

Plasma levels of IL-6, LPO, SOD, MDA, cAMP, and the levels of SERCA, NKA in myocardial tissue were determined using the corresponding ELISA kits according to the manufacturers' instructions. After color development, sample absorbances were measured at 450 nm using a fluorescence reader (THERMO USA).

(3) Western blotting

Samples containing ventricular heart tissue proteins were clarified by centrifuging at 13000×*g* for 10 min at 4 °C and the supernatants were collected. Protein concentrations were determined using a bicinchoninic acid assay. Proteins were separated using 10 % sodium dodecyl sulfate–polyacrylamide gel electrophoresis and transferred onto polyvinylidene fluoride membranes. The membranes were subsequently incubated overnight with the primary antibodies (Cx43) at 4 °C and washed three times with Tris-buffered saline (TBS) containing Tween 20 (TBST) to wash off the excess antibodies. The membranes were then incubated with horseradish peroxidase–conjugated secondary antibodies for 2 h at 23 ± 2 °C. After rewashing with TBST, enhanced chemiluminescence was used for visualization, and ImageJ (NIH Image, Bethesda, MD, United States) was used to calculate the gray values. The intensity of target proteins was normalized to that of an internal reference to determine their relative expression levels.

### *2.2.1. PK–PD association analysis of LGNXT on arrhythmias*

(1) The preparation of PD model and plasma samples

The 24 rats in the Control, Model, and LGNXT groups were fasted for 12 h but given free access to water prior to the experiment. Rats in the LGNXT group were intragastrically administered a medium dose of LGNXT (10.39 g/kg/d) for three consecutive days, whereas those in the Control and Model groups were given an equal volume of 0.9 % normal saline. Blood samples for PD analysis were collected at 5 min, 10 min, 20 min, 40 min, 1 h, 1.5 h, 2 h, 4 h, 6 h, 8 h, 12 h, and 24 h after Adr modeling, centrifuged at 13000×*g* for 10 min to separate the plasma, and stored at −80 °C. Changes in IL-6, LPO, and cAMP levels were measured using ELISA. The ability to inhibit inflammation, oxidative stress, and energy metabolism was evaluated by Δ PD% (Δ IL-6, Δ LPO, and Δ cAMP) using the following formula:

$$\Delta PD\% = (PD_{Control} - PD_{LGNX\text{-}10.39\ g/kg/d}) \,/\, (PD_{Control} - PD_{Model}) \times 100\%$$

(2) HPLC-MS/MS

Chromatographic separations were achieved using an ACQUITYTM UPLC BEH $C_{18}$ (100 mm × 2.1 mm, 1.7 μm) maintained at 30 °C with a thermostatic column oven and injection volume of 5 μL. Samples were eluted at a flow rate of 0.45 mL $min^{-1}$ using a gradient elution program of A (0.1 % formic acid: water) and B (0.1 % acetonitrile: water) as follows: 0–0.5 min, 1%–50 % B at 0.5–2 min, 50%–100 % B at 2–7 min, 100%–100 % B at 7–10 min, 100%–1% B at 10–11 min, 1%–1% B at 11–13 min.

Quantitative analysis was performed with multiple reaction monitoring (MRM), and positive/negative ion dual mode was used for detection. The MS/MS setting parameters were as follows: GAS1 50 mL/min; CAS2 50 mL/min; turbo spray temperature 500 °C; ion spray voltage 5500/–4500 V; CUR 25 L/min. MRM transitions and other parameters are summarized in Appendix A.

(3) Preparation of standard solution, quality control (QC) samples and internal standard (IS)

Accurately weigh the standard compound 10 mg, and dissolved in DMSO to prepare a 2 mg/mL mixed stock solution. The stock solution was diluted with 50 % methanol aqueous solution in different proportions to obtain mixed working solutions with different concentrations. The final mass concentrations of standard solutions were as follows: berberine, liquiritin, puerarin, methylophiopogonanone A (0.25, 0.5, 2, 8, 32, 128, 640, 800 ng/mL), trigonelline and cinnamic acid (0.5, 1, 4, 16, 64, 256, 1024, 1600 ng/

mL), tetrahydropalmatine, dehydropalingic acid, tangerine (1, 2, 8, 32, 128, 640, 3200, 4000 ng/mL). The QC samples were prepared according to the method of sample preparation (0.5, 32, 640 ng/mL for berberine, methylophiopogonanone A, liquiritin, puerarin, 1, 256, 1024 ng/mL for trigonelline and cinnamic acid, and 2, 640, 3200 ng/mL for tetrahydropalmatine, dehydropalingic acid, tangerine) at low, medium and high concentrations. IS stock solutions were prepared by dissolving naringin in methanol to 2 μg/mL. All standard solutions were stored at 4 °C before use.

(4) The preparation of PK model and plasma sample

The 16 rats in Control and LGNXT groups were also fasted for 12 h but were provided free access to water prior to commencing experiments. Rats in both groups were administered 10.39 g/kg/d LGNXT for three consecutive days. The methods of modeling and collection of plasma samples were similar to those used for PD. 20 μL of IS solution was added to 100 μL of blank plasma and vortex-mixed for 1 min. Then, 500 μL of methanol was added, vortexed for 5 min, centrifuged at 13000×*g* at 4 °C for 15 min, and dried at 30 °C under a stream of $N_2$. Then reconstituted with 200 μL of methanol, vortexed for 5 min, centrifuged at 13000×*g* for 15 min. Lastly, the supernatant (5 μL) was injected for HPLC-MS/MS analysis.

(5) Method validation for PK study

Method validation was performed according to the Pharmacopoeia of the People's Republic of China, and FDA Bioanalytical Method Validation guidelines. The current HPLC-MS/MS method was validated for selectivity, linearity, lower limit of quantification (LLOQ), intra- and inter-day precision, accuracy, matrix effect (MF), recovery, and stability.

(6) PK–PD association to determine the pharmacodynamic substances in LGNXT

The most direct link between PK and PD was made by the simultaneous measurements of effect and concentration at the effect site (Fig. 2). Combining the "effect-time" curve constructed using the plasma PD markers and the "dose-time" curve constructed using the blood concentration of the potential pharmacodynamic substances in LGNXT, the PD marker–time curve of active ingredients was finally obtained. The active ingredients closely related to inhibiting inflammation, oxidative stress, and energy metabolism were identified to further verify the mechanisms and pharmacodynamic substances of LGNXT for the management of arrhythmias.

### *2.3. Statistical analysis*

Measurement data are expressed as the mean ± standard error of the mean. One-way ANOVA was used for comparison between groups (SPSS, Inc., Chicago, IL, USA). $P < 0.05$ indicates statistical significance. Chromatograms were obtained using Masslynx software (Version 4.1; Waters Company) and the peak area was calculated. The area under the plasma concentration–time curve (AUC) from time 0–24 h ($AUC_{0-24\ h}$), AUC extrapolated to infinity ($AUC_{0-\infty}$), peak concentration (Cmax), elimination half-life ($t_{1/2}$), and time to achieve Cmax (Tmax) were calculated based on the actual time of blood collection using DAS2.0. Graphs were plotted using Graph Pad Prism 8.0.

## 3. Results

### *3.1. LGNXT significantly reduced Adr-induced arrhythmias*

(1) Onset and duration of arrhythmias

Adr dose onset and duration of arrhythmias are shown in Fig. 4A and B. Arrhythmias induced by Adr were mainly ventricular arrhythmias (Fig. 3A–F). With an increase in the cumulative dose of Adr, the type of arrhythmia changed from ventricular tachyarrhythmia to both ventricular premature beats and sinus bradycardia, resulting in a gradual prolongation of duration. Meanwhile, the onset time of arrhythmias gradually advanced and the duration gradually prolonged, indicating that arrhythmia severity was proportional to Adr levels. Treatment with LGNX-10.39 g/kg/d and Meto could delay the onset of arrhythmia ($p < 0.05$, 0.01) with similar effects. All other groups except the LGNX-5.19 g/kg/d group exhibited a markedly shortened time to arrhythmia. Treatment with LGNX-20.77 g/kg/d and LGNX-10.39 g/kg/d exhibited an antiarrhythmic effect equivalent to that of Meto (at 32 μg/kg, 64 μg/kg, and 128 μg/kg) ($p > 0.05$). Therefore, LGNXT, especially the medium dose used in this study, could significantly reduce Adr-induced arrhythmias.


**Fig. 2.** Schematic diagram of the dose-time-effect relationship represented by the PK and PD models. PD: pharmacodynamics; PK: pharmacokinetics; EC: effect-site concentration; CP: plasma concentration.


**Fig. 3. Common types of Adr-induced arrhythmias**. A: Normal ECG; B: Sinus bradycardia; C: Single premature ventricular; D: Bigamy; E: Paroxysmal ventricular tachycardia; F: Atrioventricular block.

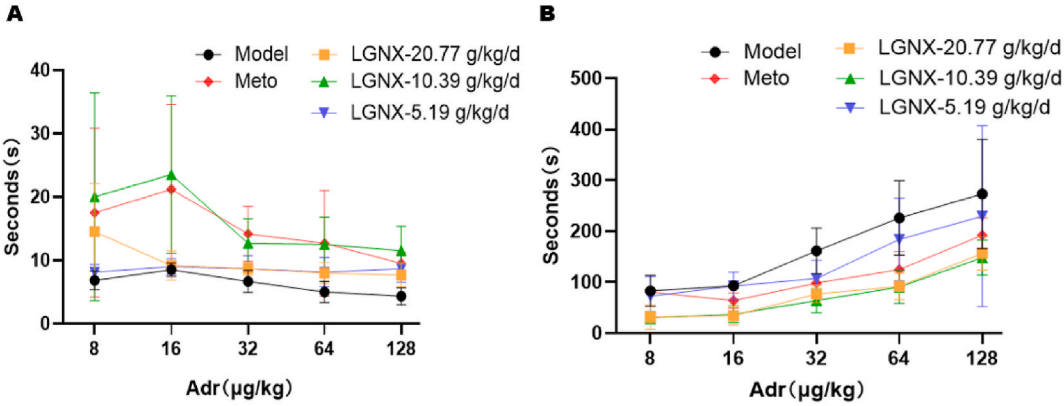


**Fig. 4. Relationship between Adr dose and the initial time (A) and duration (B) of arrhythmias. ($\bar{x} \pm s$, n = 8).**

(2) QRS duration and QTc interval

The effects of LGNXT on QRS duration and QTc interval were investigated (Fig. 5A and B). Arrhythmia caused by Adr had the effect of prolonging ventricular depolarization (QRS interval). After the prophylactic administration of LGNXT and metoprolol, respectively, the QTc interval was shortened with no significant effect on the QRS interval. There was no significant difference between the LGNX-20.77 g/kg/d group and the LGNX-10.39 g/kg/d group compared with the nonmodeled rats (at 8 μg/kg, 16 μg/kg, and 32 μg/kg). However, rats in the LGNX-5.19 g/kg/d and Meto groups were at risk of shortening of the QT interval when high doses were administered (32 μg/kg, 64 μg/kg, 128 μg/kg). Thus, LGNXT could reduce QT dispersion in rats with arrhythmia without new arrhythmogenic effects.

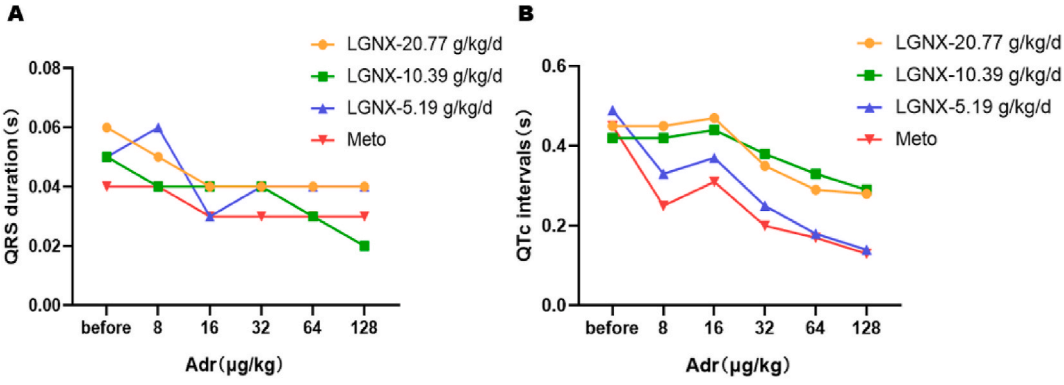


**Fig. 5. QRS duration and QTc intervals at baseline, and changes with increasing adrenaline dose ($\bar{x} \pm s$, n = 8).**

### 3.2. LGNXT ameliorated arrhythmias by regulating SOD, MDA, and LPO levels

The expression of the oxidative stress response–related molecules, SOD, MDA, and LPO in the Model group changed 0.9-fold, 1.1-fold, and 1.1-fold, respectively, compared with that in the Control group (Table 1, Fig. 6). Except for the LGNX-5.19 g/kg/d group, the serum MDA and LPO levels were reduced markedly and SOD level was increased in all other groups ($p < 0.05$, 0.01). There was no significant difference between the LGNX-10.39 g/kg/d and LGNX-20.77 g/kg/d groups compared with the Control group ($p > 0.05$). Thus, inhibition of oxidative stress may be an essential mechanism leading to the antiarrhythmic effect of LGNXT.

### 3.3. LGNXT ameliorated arrhythmias by regulating IL-6 and cAMP levels

IL-6 and cAMP levels in the Model group increased significantly ($p < 0.05$) compared with those in the Control group (Table 2, Fig. 7). The administration of LGNXT and Meto abolished the effect of Adr on the increase in IL-6 and cAMP levels ($p < 0.05$). However, only LGNX-10.39 g/kg/d could significantly downregulate cAMP levels to normal ($p > 0.05$). In other words, middle-dose LGNXT had the best curative effect. Thus, LGNXT may exert antiarrhythmic effects by inhibiting inflammatory response and energy metabolism.

### 3.4. LGNXT ameliorated arrhythmias by regulating NKA and SERCA levels

SERCA and NKA activities are shown in Table 3 and Fig. 8. LGNX-10.39 g/kg/d and Meto could significantly increase SERCA and NKA levels ($p < 0.05$, 0.01) compared with that in the Model group, whereas LGNX-20.77 g/kg/d could only increase SERCA levels ($p < 0.01$). NKA and SERCA levels approached normal after treatment with LGNXT and Meto, suggesting that LGNXT may exert its antiarrhythmic effect by correcting abnormal ion channels.

#### 3.4.1. LGNXT ameliorated arrhythmias by regulating myocardial Cx43 expression

Cx43 protein expression levels were determined using WB (Table 4, Fig. 9). Myocardial Cx43 expression in the Model group increased significantly compared with that in the Control group ($p < 0.01$), whereas it decreased significantly after treatment with LGNXT and Meto ($p < 0.01$). No significant differences in Cx43 expression were found among the LGNXT groups ($p > 0.05$).

### 3.5. PD assessments of IL-6, LPO, and cAMP

Pharmacodynamics is a study that quantitatively describes the changes in drug effects *in vivo* over time. The dynamic changes in IL-6, LPO, and cAMP within 24 h showed that LGNXT had a significant effect on inhibiting the inflammatory response, oxidative stress, and energy metabolism due to arrhythmia, and that it had a rapid onset and prolonged effect (Fig. 10).

Δ IL-6, Δ LPO, and Δ cAMP were calculated using the formula shown in Fig. 11, which was further adopted to analyze the PK–PD association. The effect of LGNXT in reducing IL-6 was rapid and peaked at approximately 1 h. A shoulder peak was observed at about 2 h, which gradually decreased and stabilized. The inhibition of LPO was strong and persistent, and peak inhibition was attained at approximately 1 h, 4 h, and 12 h. The Δ cAMP curve showed a bimodal phenomenon, reaching the peak at approximately 40 min and 2 h; LGNXT had the strongest inhibitory ability and decreased rapidly. However, after 6 h, there was a slight upward trend, which may be related to drug redistribution.

So far, we have verified the clinical efficacy of LGNXT on arrhythmias and revealed its pharmacodynamic mechanisms via modulating the inflammatory response, oxidative stress, and energy metabolism. Next, we will focus on the PD–PK association to clarify the pharmacological targets of berberine, trigonelline, tetrahydropalmatine, liquiritin, methylophiopogonanone A, puerarin, dehydropachymic acid, nobiletin, and cinnamic acid, and further verify the pharmacodynamic substances and the antiarrhythmic mechanism of LGNXT.

#### 3.5.1. HPLC-MS/MS method validation

Typical MRM chromatograms of blank plasma, blank plasma spiked with the standard compound and IS, and plasma samples obtained after the intragastric administration of LGNXT are shown in Appendix B. No interfering peaks were detected in the chromatograms of blank plasma samples, and well-defined peaks were observed in the chromatograms of plasma samples spiked with the target analytes. The analytical curve was linear and the correlation coefficients were greater than 0.9901 (Appendix C). Intra-day

**Table 1**
Effects of LGNXT on SOD, MDA, and LPO levels in rats with arrhythmia ($\bar{x} \pm s$, n = 8).

| Group | SOD (U/L) | MDA (nmol/L) | LPO (nmol/L) |
|---|---|---|---|
| Control | 173.32 ± 14.51 | 3.97 ± 0.26 | 723.45 ± 15.17 |
| Model | 145.71 ± 11.09** | 4.37 ± 0.18* | 802.40 ± 32.74** |
| LGNX-20.77 g/kg/d | 155.67 ± 17.38* | 4.04 ± 0.27 | 753.32 ± 29.72$^{\triangle\triangle}$ |
| LGNX-10.39 g/kg/d | 167.26 ± 12.81$^{\triangle\triangle}$ | 3.85 ± 0.34$^{\triangle\triangle}$ | 742.73 ± 29.83$^{\triangle\triangle}$ |
| LGNX-5.19 g/kg/d | 164.97 ± 14.98$^{\triangle}$ | 3.94 ± 0.29$^{\triangle}$ | 745.42 ± 34.00$^{\triangle\triangle}$ |
| Meto | 164.44 ± 12.04$^{\triangle}$ | 3.66 ± 0.28$^{\triangle\triangle}$ | 743.04 ± 18.48$^{\triangle\triangle}$ |

*$p < 0.05$, **$p < 0.01$ vs. the Control group; $^{\triangle}p < 0.05$, $^{\triangle\triangle}p < 0.01$ vs. the Model group.

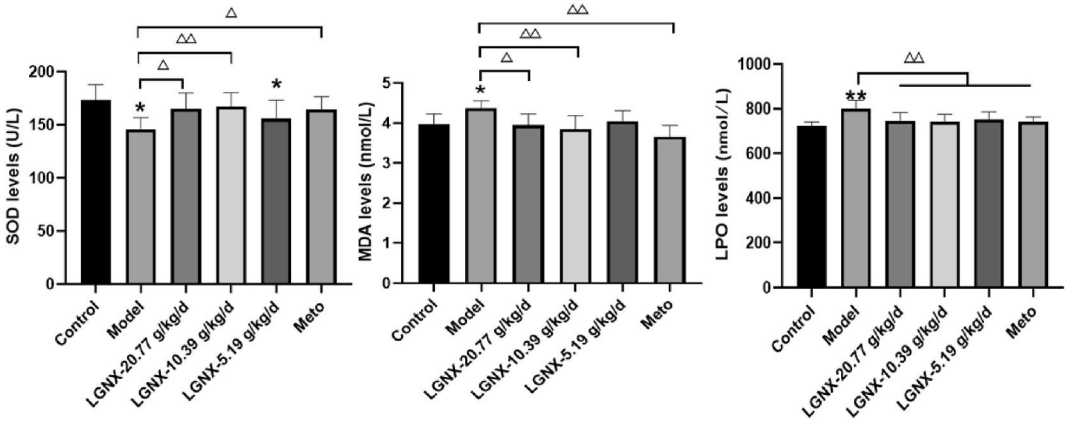


**Fig. 6. LGNXT reduced the expression of MDA and LPO and increases the low expression of SOD in arrhythmic rats. ($\bar{x} \pm s$, n = 8).**

**Table 2**
Effects of LGNXT on IL-6 and cAMP levels in rats with arrhythmia ($\bar{x} \pm s$, n = 8).

| Group | IL-6 (ng/L) | cAMP (nmol/L) |
|---|---|---|
| Control | 109.68 ± 4.28 | 7.07 ± 0.13 |
| Model | 151.14 ± 10.11** | 9.55 ± 0.44** |
| LGNX-20.77 g/kg/d | 122.74 ± 6.32*△△ | 7.91 ± 0.27**△△ |
| LGNX-10.39 g/kg/d | 111.76 ± 4.67△△ | 7.37 ± 0.65△△ |
| LGNX-5.19 g/kg/d | 120.86 ± 5.16*△△ | 7.82 ± 0.32*△△ |
| Meto | 118.34 ± 7.92△△ | 7.61 ± 0.28△△ |

*$p < 0.05$, **$p < 0.01$ vs. the Control group; △$p < 0.05$, △△$p < 0.01$ vs. the Model group.

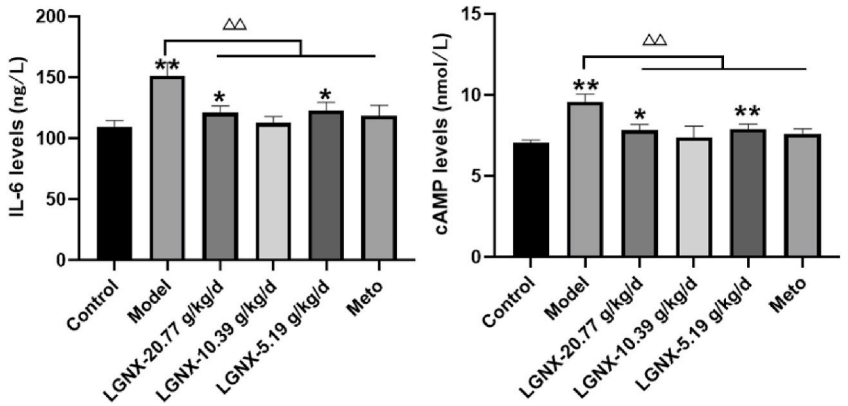


**Fig. 7. LGNXT reduced IL-6 and cAMP expression in rats with arrhythmia ($\bar{x} \pm s$, n = 8).**

**Table 3**
Effects of LGNXT on NKA and SERCA in rats with arrhythmia ($\bar{x} \pm s$, n = 8).

| Group | NKA (U/mL) | SERCA (U/mL) |
|---|---|---|
| Control | 11.52 ± 0.27 | 20.61 ± 1.85 |
| Model | 9.82 ± 1.11** | 17.63 ± 1.96** |
| LGNX-20.77 g/kg/d | 10.29 ± 1.17* | 19.41 ± 2.1 |
| LGNX-10.39 g/kg/d | 11.29 ± 0.38△△ | 21.1 ± 1.43△△ |
| LGNX-5.19 g/kg/d | 10.59 ± 0.87 | 20.44 ± 0.95△△ |
| Meto | 11.03 ± 0.74△ | 19.99 ± 1.22△ |

*$p < 0.05$, **$p < 0.01$ vs. the Control group; △$p < 0.05$, △△$p < 0.01$ vs. the Model group.

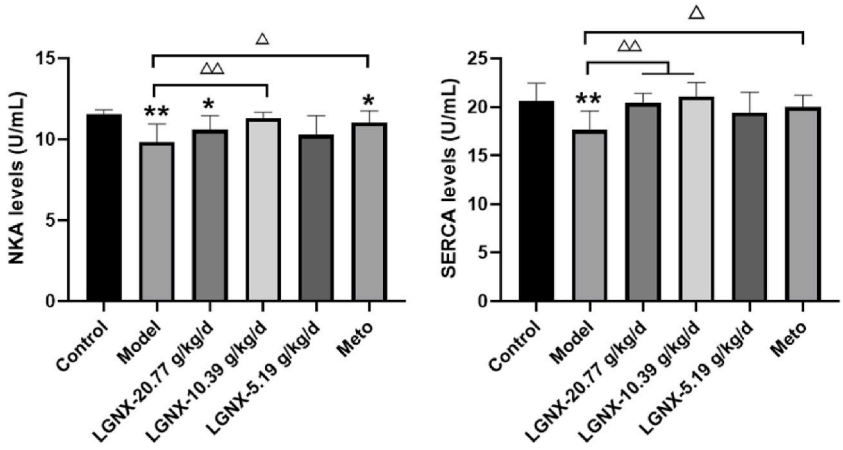


**Fig. 8. LGNXT increased NKA and SERCA expression in rats with arrhythmia ($\bar{x} \pm s$, n = 8).**

**Table 4**
Effect of LGNXT on myocardial Cx43 expression in the rat model of arrhythmia ($\bar{x} \pm s$, n = 8).

| Group | Cx43/GAPDH |
|---|---|
| Control | 0.20 ± 0.05 |
| Model | 0.76 ± 0.06** |
| LGNX-20.77 g/kg/d | 0.49 ± 0.02**△△ |
| LGNX-10.39 g/kg/d | 0.34 ± 0.04*△△ |
| LGNX-5.19 g/kg/d | 0.65 ± 0.07** |
| Meto | 0.49 ± 0.05**△△ |

*$p < 0.05$, **$p < 0.01$ vs. the Control group; △$p < 0.05$, △△$p < 0.01$ vs. the Model group.

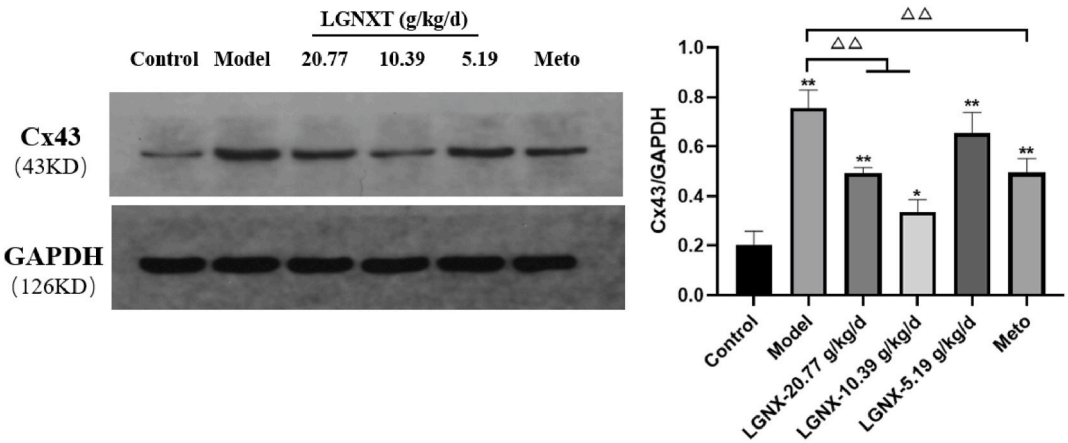


**Fig. 9. Western blots of Cx43 in each group ($\bar{x} \pm s$, n = 8).**

precision ranged from 1.05 % to 10.93 % for blood samples and inter-day precision ranged from 1.75 % to 14.79 %. The accuracy was between −0.50 % and 0.23 %, which was acceptable at the evaluated levels (Appendix D). The MF was 85%–98 %, which showed values less than 13 %, and sample recovery was 81%–97 % with a relative standard deviation of no more than 13 %, indicating that the matrix effect could be ignored and the established method had a good recovery rate for analyte extraction. Stability verification results showed that the samples could maintain stable quality in the above conditions (Appendix E).

### *3.5.2. Comparative PK behaviors among the 9 potential pharmacodynamic substances*

The validated method was further applied for PK analysis following the intragastric administration of LGNXT to rats at a dose of 10.39 g/kg/d. The mean "dose-time" profiles of the 9 potential pharmacodynamic substances are depicted in Fig. 12 and the

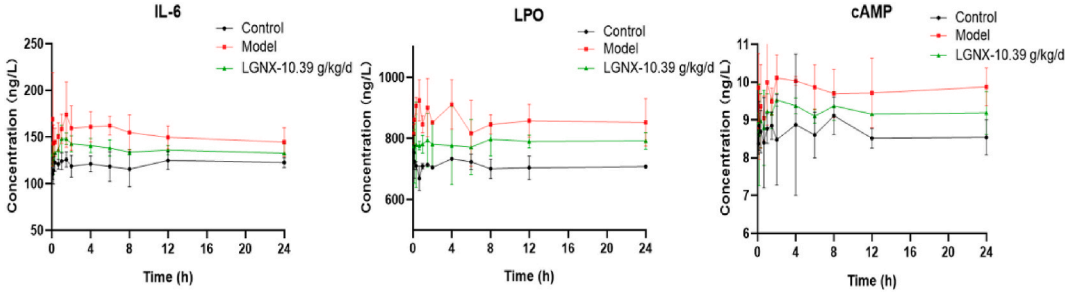


**Fig. 10. "Effect-time" curves of IL-6, LPO, and cAMP ($\bar{x} \pm s$, n = 6).**

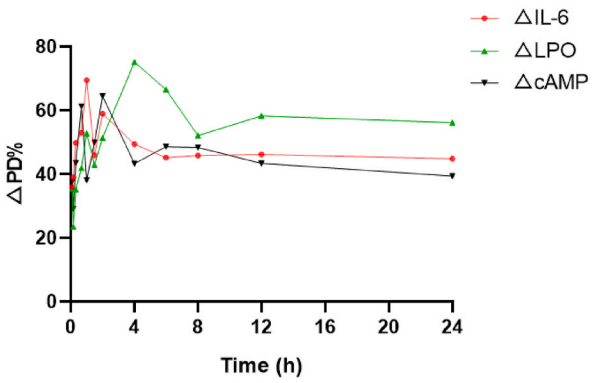


**Fig. 11.** Time curves of Δ IL-6, Δ LPO, and Δ cAMP
(ΔPD% = [$PD_{Control}$ − $PD_{LGNX\text{-}10.39\ g/kg/d}$ ]/[$PD_{Control}$ − $PD_{Model}$] × 100 %).

corresponding PK parameters are listed in Table 5. All analytes were rapidly absorbed and the Tmax values ranged from 0.17 to 1.5 h. Among the detected analytes, trigonelline, tetrahydropalmatine, dehydropachymic acid, nobiletin, and cinnamic acid, which were rapidly metabolized in the plasma, were found at prominently higher exposure levels. Berberine and methylophiopogonanone A had long $t_{1/2}$ but lower exposure levels due to low polarity and poor absorption. The $t_{1/2}$ of liquiritin, dehydropachymic acid, and puerarin could be maintained at about 7–8 h, and showed a relatively fine absorption and a higher level of exposure *in vivo*. These results showed the extensive uptake of LGNXT in the blood and the slow distribution after intragastric administration. And to a certain extent, the changes of pharmacokinetic parameters of the compounds in the LGNXT illustrated the synergistic or antagonistic effect between components in the formula. The advantage of compound Chinese medicine lies in the compatibility of different Chinese medicines so as to regulate the body as a whole.

On one side, the PK study showed great significance on the study of pharmacokinetic process of active components in LGNXT. In addition, this section played a guiding role on the deeply study of PK–PD association, to further verify the pharmacodynamic substances and the antiarrhythmic mechanism of LGNXT.

### *3.5.3. PK–PD association*

As shown in Fig. 13, the Emax of IL-6 and the Cmax of methylophiopogonanone A, nobiletin, and trigonelline were consistent. The peak effect at 2 h was likely related to cinnamic acid and nobiletin. The Tmax values of berberine and dehydropalingic acid were slightly earlier than the peak effect of 1 h; the Tmax values of liquiritin and puerarin were 1.5 h, whose Cmax lagged behind the peak time. The anti-inflammatory response of LGNXT tended to be stable after 4 h, which may be related to dehydropalingic acid with a longer $t_{1/2}$ and larger AUC. Therefore, trigonelline, methylophiopogonanone A, nobiletin, cinnamic acid, liquiritin, dehydropolisic acid, berberine, and puerarin could be regarded as the main pharmacodynamic substances for inhibiting the inflammatory response in arrhythmias.

As shown in Fig. 14, dehydropalingic acid and methylophiopogonanone A had peak concentrations at 4 h, which were related to drug distribution-reabsorption or enterohepatic circulation. The peak effect at 1 h may be related to trigonelline, nobiletin, and methylophiopogonanone A. The Tmax values of dehydropalingic acid and berberine were slightly earlier than 1 h, indicating a certain lag effect. The plasma concentration of puerarin showed a rising trend within 1 h, promoting the antioxidant effect of LGNXT. Additionally, Δ LPO had a relatively stable peak effect at 12 h, which may be related to the longer $t_{1/2}$ and higher AUC of dehydropalingic acid.

The Emax of cAMP appeared at 2 h, when the level of dehydropalingic acid showed an increase. Due to the oxidative metabolism of cinnamaldehyde and enterohepatic circulation, the levels of cinnamic acid and nobiletin peaked again. Liquiritin and puerarin only

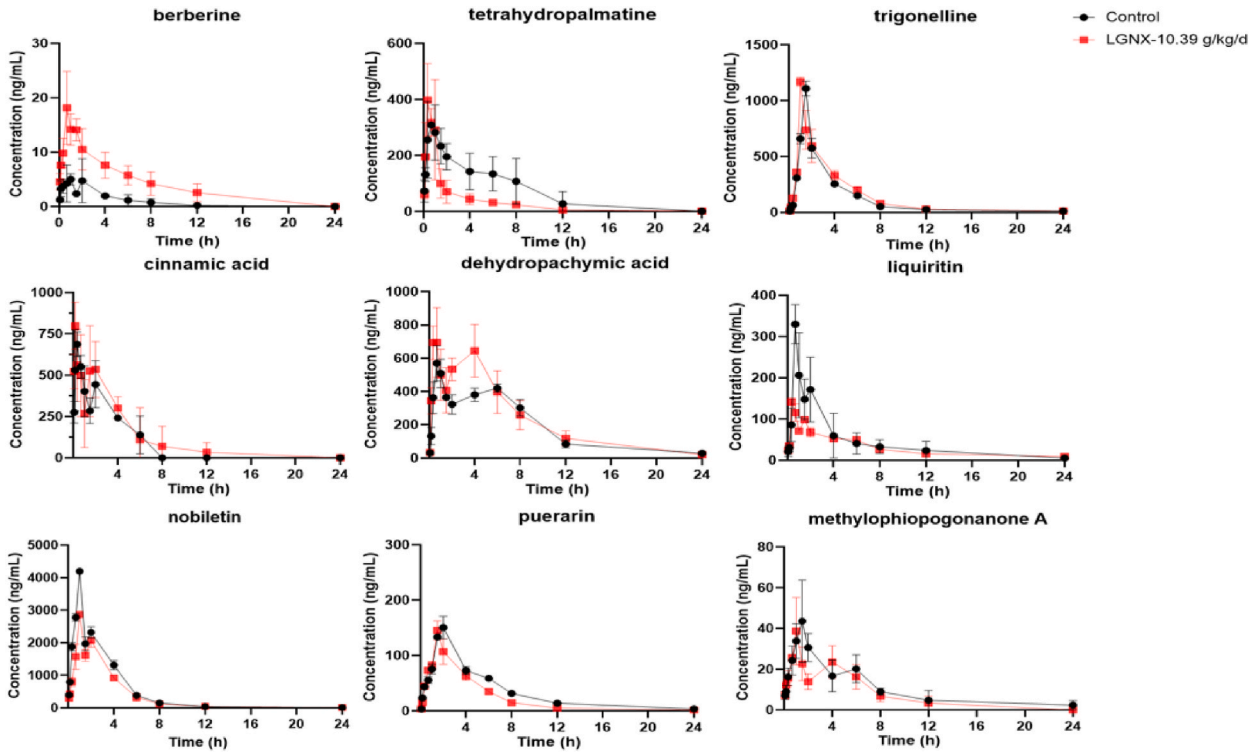


**Fig. 12.** Mean "dose-time" profiles of the 9 potential pharmacodynamic substances after the intragastric administration of LGNXT in rats with arrhythmia (n = 6).

**Table 5**
Pharmacokinetic parameters of the 9 analytes after the intragastric administration of LGNXT in rats with arrhythmia (n = 6).

| Analyte | $AUC_{(0\rightarrow t)}$ (μg/L·h) | $AUC_{(0\rightarrow\infty)}$ (μg/L·h) | $MRT_{(0\rightarrow t)}$ (h) | $MRT_{(0\rightarrow\infty)}$ (h) | $t_{1/2}$ (h) | Tmax (h) | Cmax (ng/ml) |
|---|---|---|---|---|---|---|---|
| berberine | 91.12 ± 52.94 | 161.81 ± 12.77 | 4.26 ± 0.61 | 14.72 ± 7.88 | 11.91 ± 5.00 | 0.61 ± 0.42 | 30.95 ± 28.61 |
| trigonelline | 3859.95 ± 46.44 | 3887.51 ± 60.35 | 4.18 ± 0.19 | 4.53 ± 0.33 | 2.58 ± 0.24 | 1.00 ± 0.00 | 1170.86 ± 39.78 |
| liquiritin | 708.20 ± 49.16 | 747.18 ± 83.59 | 6.75 ± 0.84 | 10.72 ± 5.65 | 7.14 ± 2.06 | 0.33 ± 0.00 | 141.62 ± 8.69 |
| methylophiopogonanone A | 632.62 ± 33.65 | 633.68 ± 33.99 | 6.52 ± 2.09 | 9.01 ± 5.50 | 7.15 ± 4.70 | 1.67 ± 0.29 | 86.50 ± 19.40 |
| tetrahydropalmatine | 848.66 ± 54.32 | 881.49 ± 47.22 | 2.91 ± 0.54 | 3.66 ± 0.54 | 3.26 ± 1.13 | 0.28 ± 0.10 | 420.96 ± 97.71 |
| puerarin | 602.59 ± 69.38 | 615.07 ± 87.43 | 4.19 ± 0.83 | 4.76 ± 1.55 | 7.06 ± 4.39 | 1.50 ± 0.00 | 145.28 ± 17.00 |
| nobiletin | 9891.65 ± 40.69 | 9921.32 ± 87.64 | 3.24 ± 0.11 | 3.28 ± 0.19 | 6.32 ± 0.89 | 1.00 ± 0.00 | 2868.89 ± 22.56 |
| dehydropachymic acid | 6234.31 ± 41.22 | 6336.63 ± 55.44 | 5.93 ± 0.44 | 6.42 ± 0.49 | 7.62 ± 2.05 | 0.44 ± 0.19 | 782.32 ± 158.00 |
| cinnamic acid | 2007.62 ± 73.26 | 7692.83 ± 68.43 | 2.64 ± 1.31 | 2.48 ± 2.81 | 4.78 ± 1.67 | 0.17 ± 0.00 | 799.93 ± 142.32 |

appeared at the peak concentration. The dose-effect relationship of berberine and dehydropalingic acid was consistent at 40 min. At the same time, plasma concentrations of trigonelline, methylophiopogonanone A, nobiletin, and puerarin were increasing and the Tmax of tetrahydropalmatine, liquiritin, and cinnamic acid were achieved slightly sooner than the peak effect, showing a certain degree of lag effect on the inhibition of energy metabolism. After 6 h, the inhibition of energy metabolism increased gradually, which may be related to the longer $t_{1/2}$ and larger AUC of dehydropalmic acid (Fig. 15).

## 4. Discussion

### *4.1. Mechanism of Adr-induced arrhythmias*

(1) Adr induced arrhythmia via energy metabolism

The Adr-induced arrhythmia model is established by stimulating the sympathetic nerves to release catecholamines, which act on the corresponding adrenergic receptors in myocardial cell membranes and elicit several downstream signaling events [11]. The β1 subtype is predominant in the ventricular myocardium, and activation of the β1 receptor affects the Gs/AC/cAMP/PKA/L-$Ca^{2+}$ signaling pathway, inducing energy metabolism and leading to intracellular $Ca^{2+}$ oscillation, induction of delayed post-depolarization,

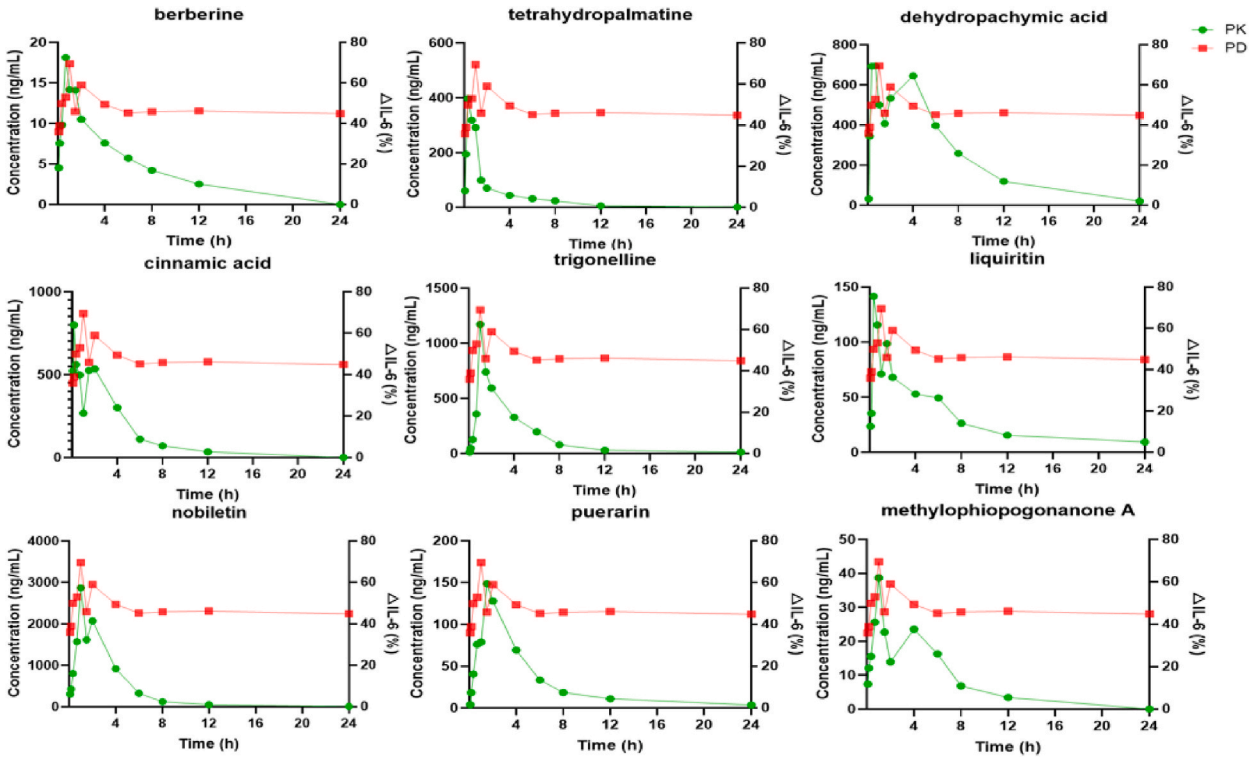


**Fig. 13.** 24-h plasma "dose-time-IL-6" change trend of the 9 analytes.

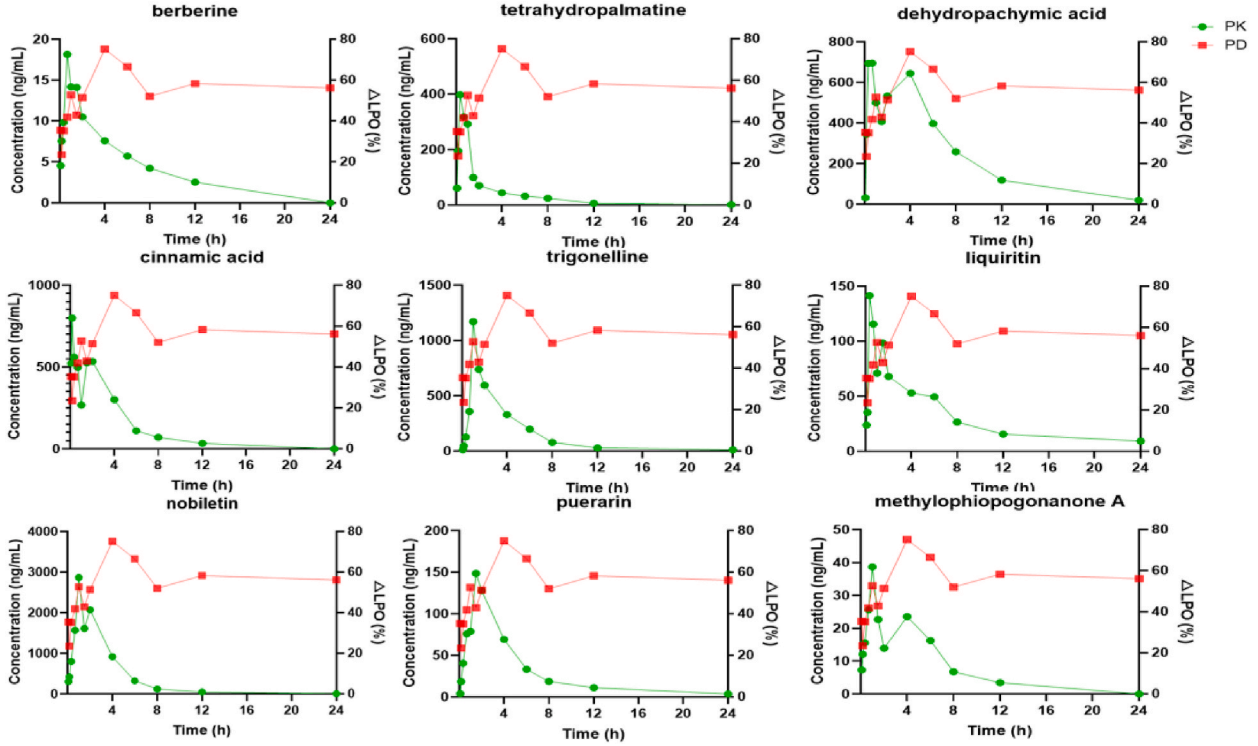


**Fig. 14.** 24-h plasma "dose-time-LPO" change trend of the 9 analytes.

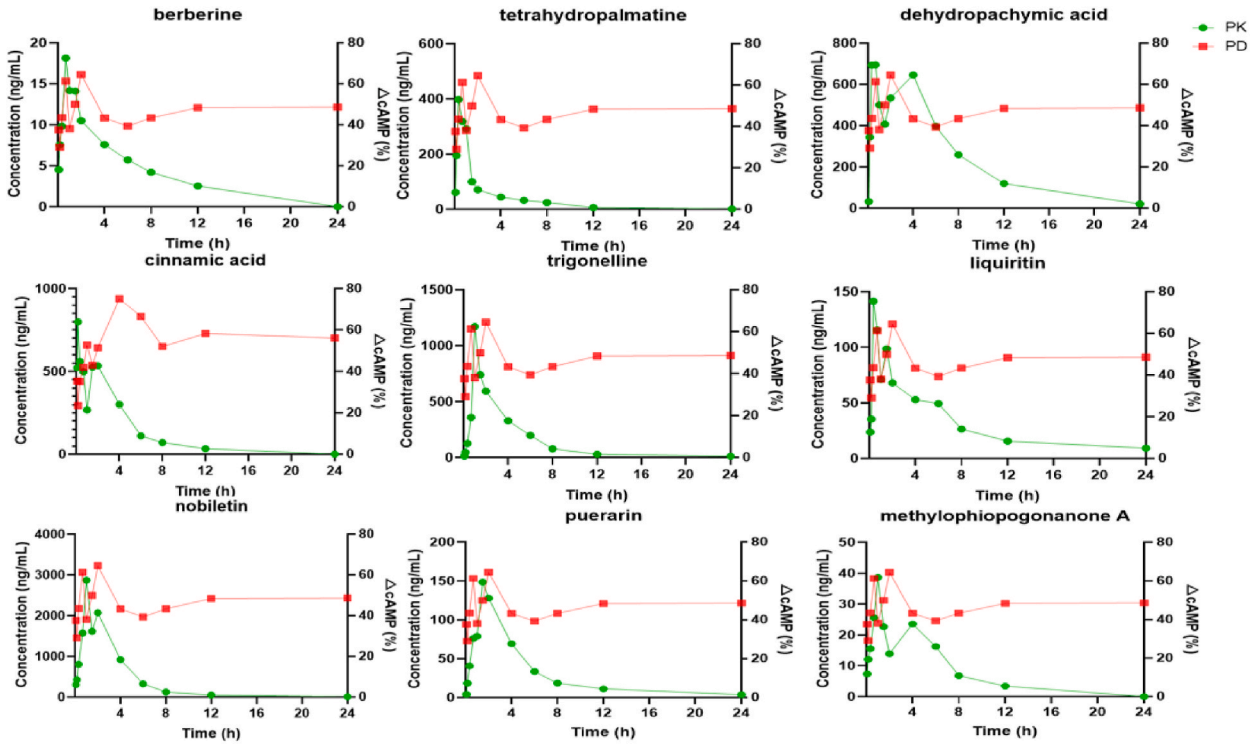


**Fig. 15.** 24-h plasma "dose-time-cAMP" change trend of the 9 analytes.

and triggering of electrical activity [12].

(2) Adr induction led to oxidant/antioxidant imbalance causing arrhythmia

It has been documented that large dose of catecholamines, experimentally, can promote the formation of oxyradicals and other oxidants [8,13–15]. The excess Adr autoxidizes to adrenochrome, which stimulates adrenal oxidation, thereby increasing the number of free radicals [16], leading to an oxidant/antioxidant imbalance [17]. The net result is the change in the activity of membrane components, destruction of the structural integrity of membranes, and an increase in membrane fluidity and calcium ion permeability. At the same time, the activities of various enzymes in the mitochondrial respiratory chain were decreased, the synthesis of adenosine triphosphate (ATP) was significantly reduced, and the sarcoplasmic reticulum (SR) was damaged. This process led to the abnormal distribution of ions inside and outside the cell, which manifested as intracellular $Ca^{2+}$ overload, disordered conduction of electrical activity, and reentrant excitation, resulting in severe arrhythmia [18]. Thus, there is a possibility that Adr-induced arrhythmias are mediated due to oxidative stress, which, in turn, leads to lipid peroxidation [15].

(3) Adr causes an inflammatory response and induces arrhythmias

Recent advances in the pathophysiology of cardiac arrhythmias indicate that inflammation can facilitate the development of arrhythmias by interfering either with electrical remodeling or the function of different cardiac ion channels. Catecholamines can activate MAPK/ERK/JNK, causing changes to cytokines including IL-6 [19] and increasing the inflammatory response [20]. It can modulate the expression and/or function of several cardiac ion channels leading to either a gain or loss of function. Additionally, the release of inflammatory factors can lead to oxidative stress, thereby altering membrane permeability and protein configurations [21].

In terms of modern social living environment, the pressure of all aspects of the population is deepened, and anxiety attacks is increased, promoting sympathetic overexcited, which meets the needs of clinical arrhythmia research. Besides, modern studies have established that enhanced sympathetic tone decreases action potential duration and increases sarcoplasmic reticular calcium leak and triggered activity. Therefore, the study was carried out by establishing an arrhythmia rat model by injection of Adr. As stated above, inflammation, oxidative stress, and abnormal energy metabolism can lead to abnormalities in ion homeostasis and the higher production/release of certain molecules due to dysfunctional cell membranes and functional modifications [15], and may be the underlying mechanisms of Adr-induced arrhythmias.

### 4.2. Mechanism of treating arrhythmia using LGNXT

(1) Abnormal distribution and expression of Cx43 induced by inflammation, oxidative stress, and energy metabolism

The expression and localization of intercellular connexin largely determine electrical conduction velocity [22]. Cx43 is the predominant gap junction protein in the myocardium that is involved in the control of cell-to-cell communication. It modulates the electrical coupling of cardiac myocytes and stabilizes cell membrane structure and function [23–25]. Some signaling systems alter the gating properties of gap junctions to cause arrhythmias by inducing Cx43 phosphorylation status [26,27]. Increased oxidative stress products (MDA, LPO) together with excessive oxyradicals attack the cell membranes [17], leading to Cx43 downregulation, which results in abnormal conduction and an increased propensity for reentrant arrhythmias [28]. cAMP can act on the AC/cAMP/PKA/$Ca^{2+}$ signaling pathway and activate calmodulin/calmodulin protein kinase II (CaM/CaMKII). Whereas phosphorylated CaMKII directly interacts with Cx43 and dephosphorylates the 368 loci in the C-terminus of the Cx43 protein, leading to lateral remodeling [29,30], and resulting in a loss of coupling between cardiomyocytes [31,32]. IL-6 can aggravate Cx43 decoupling, thereby affecting atrial conduction velocity, enhancing reentry currents, and causing an uneven action potential duration, thereby promoting the onset of arrhythmias [33].

(2) Reduced SERCA and NKA activity induced by inflammation, oxidative stress, and energy metabolism

Ion channels control electrical excitability in living cells. Myocardial cells almost always rely on aerobic metabolism; therefore, inflammation, energy metabolism, and oxidative stress can contribute to cardiomyocyte ischemia [15]. Aerobic metabolism in cardiac cells is converted to anaerobic metabolism and ATP levels are significantly reduced, thereby affecting the function of enzymes, such as SERCA, and the NKA pump.

SERCA mediates the reuptake of $Ca^{2+}$ from the cytosol into the SR via SERCA2a (a SERCA subtype widely distributed in the myocardium) [34], which leads to cardiac muscle relaxation [22]. Oxidative stress results in the generation of a large amount of ROS, insufficient SOD scavenging, and oxidation of the sulfonyl groups of SERCA, which collectively lead to the inhibition of SERCA2a [15,35], an increase in basal cytoplasmic $Ca^{2+}$ overload [36], and prolongation of the time for $Ca^{2+}$ re-entry into the SR when the cardiomyocytes are excited. Thus, the reduction of SERCA2a activity is a common cellular mechanism underlying impaired contractile function and arrhythmogenesis.

The primary function of NKA is to maintain the difference in ion concentrations inside and outside the membrane, and to maintain the balance of electrolytes and fluids [37,38]. On one hand, inhibiting NKA activity and acidic metabolites from anaerobic metabolism is necessary and also sufficient to develop hyperkalemia, which can reduce the resting potential and increase cardiomyocyte excitability [39]. On the other hand, the inhibition of NKA can lead to the activation of CaMKII, resulting in the downstream effects on the

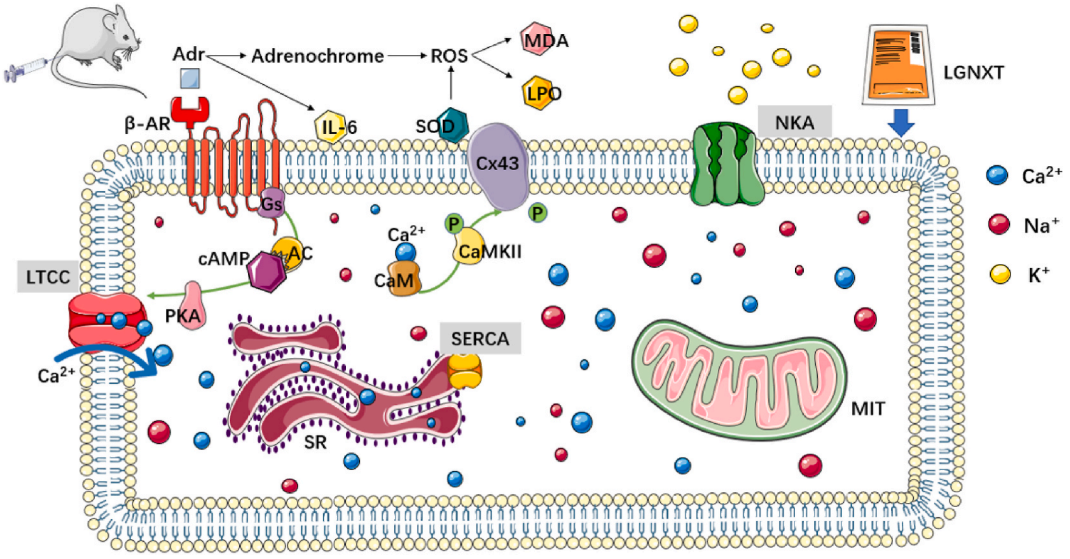


**Fig. 16.** Mechanisms of LGNXT in the treatment of arrhythmias
In the physiological state, NKA transports 2 $K^+$ into the cell and 3 $Na^+$ out of the cell in the presence of ATP. SERCA absorbs $Ca^{2+}$ from the cell into the SR in the presence of ATP to maintain homeostasis of intracellular $Ca^{2+}$ ions. After Adr injection, on the one hand, it directly bound to the receptor on G protein and activated the AC/cAMP/PKA/$Ca^{2+}$ pathway and the LTCC channel, causing $Ca^{2+}$ influx. On the other hand, it induced oxidative stress and inflammatory response, enhanced anaerobic metabolism, and inhibited the functioning of energy-dependent ion channels [NKA, SERCA], causing disorders in the membrane structure, severe intracellular calcium overload, and extracellular hyperkalemia, thereby promoting arrhythmia.

voltage-gated $Na^{+}$ current and L-type $Ca^{2+}$-channel currents (LTCC) [37]. Prolongation of action potentials can cause early after-depolarization and induce ventricular tachycardia that may progress to ventricular fibrillation [28]. These findings are in line with the findings from our previous study (Chen et al., 2020).

(3) LGNXT exerted a "membrane-stabilizing" effect to alleviate arrhythmia

In this study, an increase in Cx43 and a decrease in SERCA and NKA were observed in rats with Adr-induced arrhythmia, suggesting that the mechanism of arrhythmia was based on structural disturbances and functional modifications of cell membranes from the other side. Based on the previous discussion, the occurrence of arrhythmias and myocardial damage may significantly depend on inflammation, oxidative stress, and abnormal energy metabolism, leading to structural disorders, functional modifications, and electrical instability of cell membranes. Thus, on the one hand, changes in the structure and function of cell membranes could be considered an upstream signal leading to altered ion homeostasis and gap junction remodeling, indicating the onset of arrhythmias. On the other hand, changes in the structure and function of cell membranes could be reinforced by activating inflammatory and oxidative factors and enzymes, which are regarded as downstream events making cellular damage more complex. Therefore, this paradigm may indicate the likelihood of arrhythmias of greater severity and those that persist for the long term [15] (Fig. 16). However, LGNXT down-regulated MDA, LPO, IL-6, and cAMP; upregulated SOD, SERCA, and NKA release; and restored Cx43 coupling function. Results of our study indicated that the possible mechanisms of LGNXT included the inhibition of inflammation, oxidative stress, and abnormal energy metabolism in myocardiocytes and positively affecting ion homeostasis due to changes in the structure and function of cell membranes, thereby playing a critical role in alleviating different types of arrhythmias. The entire process can be named "membrane-stabilizing" action.

### 4.3. The PK-PD association of LGNXT

(1) Selection of PK and PD markers

Selecting the indicators of drug efficacy should be directly or highly related to the overall treatment effect, and be able to predict disease outcomes and explain treatment-induced changes in a clinical setting. As discussed, stabilizing the structure and function of cell membranes is key to treatment, whereas inhibition of inflammation, oxidative stress, and energy metabolism can help reduce symptoms. Thus, in this study, we considered these three pharmacological pathways as the foothold and chose IL-6, LPO, and cAMP as the PD markers to determine the efficacy of LGNXT in alleviating arrhythmia.

The selection of PK markers could be regarded as the process of screening the active ingredients in natural medicine and purifying the natural medicine into the prescription medicine. An ideal PK marker should show dose or exposure responsiveness and some correlation with efficacy [40]. Thus, it was essential to screen active substances which were high content *in vivo* of LGNXT based on the


**Fig. 17.** Corresponding effect targets of the 9 potential pharmacodynamic substances based on PK–PD association research
The inner layer represents the PK index, the middle layer represents the pharmacodynamic substances, and the outer layer represents the herbs that make up LGNXT. The legend shows the interaction between the pharmacological targets, pharmacodynamic substances, and herbs.

previous studies [5], and on this basis, the identified effective ingredients with IL-6-, LPO-, and cAMP-inhibitory effects on the basis of previous literature studies could be regard as the potential pharmacodynamic substances of the formula. In this study, 9 potential pharmacodynamic substances of LGNXT were screened as PK indicators.

(2) Identification of the pharmacodynamic substances and mechanisms of LGNXT

The purpose of this study was using PK–PD as a method to determine the pharmacodynamic substances through a series of active ingredient screening process. By characterizing the PK–PD behavior of the 9 potential pharmacokinetic substances, the PD marker–time curve was finally obtained. The pharmacological target of each active ingredient responsible for the antiarrhythmic mechanism of LGNXT were identified as shown in Fig. 17. Nobiletin, methylophiopogonanone A, cinnamic acid, dehydropolisic acid, trigonelline, liquiritin, berberine, and puerarin could be considered as the main pharmacodynamic substances for inhibiting the inflammatory response in arrhythmias. The mechanism of LGNXT in alleviating arrhythmia may be related to multiple signaling pathways such as the phosphoinosine-3-kinase/AKT, NF-κB, and IFN-β/TRIF pathways, which downregulate IL-6 expression and exert anti-inflammatory effects [41–45]. Methylophiopogonanone A, nobiletin, dehydropalingic acid, trigonelline, berberine, and puerarin in LGNXT exerted antiarrhythmic effects by inhibiting LPO release. The mechanism of action of LGNXT may be related to the chemical structures of its components, which [46,47]can improve the activity of antioxidant enzymes in multiple links of free-radical chain reactions, increase the amounts of molecular antioxidants, and directly scavenge free radicals, leading to the maintenance of the integrity of cell membranes and normal cellular function [48,49]. Dehydropalingic acid, cinnamic acid, liquiritin, methylophiopogonanone A, puerarin, tetrahydropalmatine, trigonelline, berberine, and nobiletin exerted antiarrhythmic effects by inhibiting the synthesis and release of cAMP. The mechanism may be attributed to prevention of intracellular $Ca^{2+}$ overload, thereby weakening myocardial contractility and improving diastolic function.

## 5. Conclusions

The findings from our study indicate that LGNXT exerts an antiarrhythmic effect by inhibiting inflammation, oxidative stress, and energy metabolism, thereby positively stabilizing the structure and remodifying the function of myocardial cell membranes. Additionally, the PD–PK association revealed that methylophiopogonanone A, berberine, trigonelline, liquiritin, puerarin, tetrahydropalmatine, dehydropachymic acid, nobiletin, and cinnamic acid directly target inflammatory, oxidative stress, and energy metabolism. Overall, our findings further elucidate the antiarrhythmic mechanism of LGNXT, which is presumed to be attributable to its pharmacodynamic substances.

## Funding

The present study was supported by the Natural Science Foundation of China (grant No. 82004329).

## Ethics approval and consent to participate

All experiments were approved by the Ethics Committee for the Use of Experimental Animals at the Institute of Radiation Medicine Chinese Academy of Medical Sciences. (Approval No.: IRM-533 DWLL-2020146; Date: September 10, 2020)

## Availability of data and materials

Data associated with the study has been deposited in https://www.jianguoyun.com/p/De0e434QvOOoCxjF3_MEIAA. The datasets used and/or analyzed during the current study are available from the corresponding author on reasonable request.

## Declaration of competing interest

The authors declare that they have no competing interests.

## Appendix C. Supplementary data

Supplementary data to this article can be found online at https://doi.org/10.1016/j.heliyon.2024.e36104.

**Appendix A**

MRM transition parameters and retention times of the 9 analytes (internal standard)

| Analyte | Parent (*m/z*) | Daughter (*m/z*) | DP (V) | CE (eV) |
|---|---|---|---|---|
| berberine | 336.2 | 320.2 | 45 | 52 |
| trigonelline | 138.0 | 121.0 | 35 | 20 |

(*continued on next page*)

**Appendix A** (*continued*)

| Analyte | Parent (*m/z*) | Daughter (*m/z*) | DP (V) | CE (eV) |
|---|---|---|---|---|
| liquiritin | 417.9 | 297.0 | −83 | −29 |
| methylophiopogonanone A | 341.1 | 206.0 | −68 | −40 |
| tetrahydropalmatine | 356.2 | 192.2 | 280 | 28 |
| puerarin | 417.0 | 297.0 | −34 | 20 |
| nobiletin | 403.0 | 373.0 | 102 | 40 |
| dehydropachymic acid | 505.3 | 465.3 | −110 | −45 |
| cinnamic acid | 146.8 | 103.9 | 32 | 10 |
| naringin | 579.2 | 271.1 | −100 | −40 |

## Appendix B. Representative extraction chromatograms of multiple-reaction monitoring (MRM) chromatograms of 10 analytes

1: berberine, 2: trigonelline, 3: puerarin, 4: methylophiopogonanone A, 5: dehydropachymic acid, 6: tetrahydropalmatine, 7: nobiletin, 8: cinnamic acid, 9: liquiritin, 10: naringin (IS); A: blank plasma, B: blank plasma + standard material + IS, C: Control group drug-containing plasma, D: LGNXT group drug-containing plasma.

**Appendix C**

The regression equation, correlation coefficient, LLOQ and linearity range of 9 analytes

| Analyte | LRE | $R^2$ | LLQQ/ng·mL$^{-1}$ | LR/ng·mL$^{-1}$ |
|---|---|---|---|---|
| berberine | y = 2.5346x+0.0163 | 0.9981 | 0.25–800 | 0.25 |
| trigonelline | y = 3.8405x+0.0069 | 0.9997 | 0.5–1600 | 0.5 |
| liquiritin | y = 1.0264x+0.0048 | 0.9968 | 0.25–800 | 0.25 |
| methylophiopogonanone A | y = 0.8944x+0.0014 | 0.9924 | 0.25–800 | 0.25 |
| tetrahydropalmatine | y = 2.7778x+0.0303 | 0.9994 | 0.5–1600 | 0.5 |
| puerarin | y = 1.4238x-0.0048 | 0.9924 | 0.25–800 | 0.25 |
| nobiletin | y = 0.4047x-0.0060 | 0.9924 | 1–4000 | 1 |
| dehydropachymic acid | y = 1.2666x+0.0040 | 0.9972 | 1–4000 | 1 |
| cinnamic acid | y = 0.0089x+0.1724 | 0.9901 | 1–4000 | 1 |

The regression equations were obtained through linear regression using the concentration (X) of the reference substance as the abscissa and the peak area ratio of each analyte to IS (Y) as the ordinate.

**Appendix D**

Intra-day precision, inter-day precision, accuracy, matrix effect, and recovery of the 9 analytes in plasma samples (n = 6)

| Analyte | Concentration (ng/ml) | Batch | Precision | | Accuracy (RE %) | MF (%) | | Recovery (%) | |
|---|---|---|---|---|---|---|---|---|---|
| | | | Intra-day (RSD%) | Inter-day (RSD%) | | Mean ± SD | RSD | Mean ± SD | RSD |
| berberine | 0.5 | 1 | 10.64 | 10.28 | 0.14 | 96.00 ± 7.80 | 8.12 | 89.00 ± 10.10 | 11.35 |
| | | 2 | 10.04 | | | 85.33 ± 9.52 | 11.16 | 94.33 ± 10.69 | 12.68 |
| | | 3 | 8.23 | | | 90.67 ± 9.35 | 10.32 | 86.67 ± 8.07 | 9.31 |
| | 32 | 1 | 9.70 | 4.88 | −0.50 | 92.63 ± 7.61 | 8.21 | 93.14 ± 6.64 | 7.13 |
| | | 2 | 7.65 | | | 92.26 ± 4.96 | 5.37 | 90.50 ± 5.28 | 5.83 |
| | | 3 | 2.97 | | | 90.77 ± 5.87 | 6.47 | 88.05 ± 4.18 | 4.75 |
| | 640 | 1 | 4.23 | 2.89 | −0.01 | 96.88 ± 1.52 | 1.57 | 96.80 ± 2.25 | 2.33 |
| | | 2 | 1.05 | | | 97.22 ± 1.56 | 1.60 | 95.08 ± 1.78 | 1.87 |
| | | 3 | 2.28 | | | 96.95 ± 1.93 | 1.99 | 96.30 ± 2.04 | 2.12 |
| trigonelline | 1 | 1 | 5.20 | 13.97 | 0.23 | 85.83 ± 8.52 | 9.92 | 96.00 ± 11.61 | 12.09 |
| | | 2 | 5.61 | | | 95.83 ± 7.81 | 8.15 | 91.50 ± 7.77 | 8.49 |
| | | 3 | 5.20 | | | 97.83 ± 9.41 | 9.62 | 95.17 ± 11.48 | 12.41 |

(*continued on next page*)

**Appendix D** (*continued*)

| Analyte | Concentration (ng/ml) | Batch | Precision | | Accuracy (RE %) | MF (%) | | Recovery (%) | |
|---|---|---|---|---|---|---|---|---|---|
| | | | Intra-day (RSD%) | Inter-day (RSD%) | | Mean ± SD | RSD | Mean ± SD | RSD |
| | 256 | 1 | 3.74 | 2.47 | −0.01 | 89.17 ± 5.51 | 6.18 | 87.48 ± 8.34 | 9.53 |
| | | 2 | 2.28 | | | 86.76 ± 6.05 | 6.98 | 88.71 ± 6.63 | 7.47 |
| | | 3 | 1.90 | | | 91.29 ± 8.64 | 9.46 | 87.07 ± 7.86 | 9.03 |
| | 1024 | 1 | 6.76 | 6.64 | 0.06 | 96.90 ± 5.57 | 5.74 | 95.67 ± 4.47 | 4.67 |
| | | 2 | 6.93 | | | 97.30 ± 5.76 | 5.92 | 96.64 ± 2.07 | 2.14 |
| | | 3 | 3.02 | | | 97.96 ± 1.28 | 1.31 | 96.23 ± 1.18 | 1.23 |
| liquiritin | 0.5 | 1 | 10.44 | 11.99 | 0.14 | 95.00 ± 10.26 | 10.80 | 87.67 ± 9.42 | 10.74 |
| | | 2 | 10.72 | | | 90.00 ± 6.20 | 6.89 | 94.33 ± 7.09 | 7.52 |
| | | 3 | 5.79 | | | 93.67 ± 9.33 | 9.96 | 87.67 ± 10.07 | 11.49 |
| | 32 | 1 | 5.38 | 5.70 | −0.03 | 95.13 ± 6.74 | 7.09 | 91.51 ± 9.28 | 10.14 |
| | | 2 | 5.87 | | | 92.13 ± 4.66 | 5.06 | 96.83 ± 5.26 | 5.43 |
| | | 3 | 3.87 | | | 90.94 ± 7.91 | 8.69 | 95.10 ± 6.42 | 6.75 |
| | 640 | 1 | 3.69 | 4.02 | 0.01 | 97.30 ± 0.89 | 0.91 | 93.56 ± 2.05 | 2.20 |
| | | 2 | 3.11 | | | 95.80 ± 3.18 | 3.32 | 94.99 ± 2.34 | 2.46 |
| | | 3 | 3.61 | | | 94.77 ± 3.60 | 3.80 | 95.69 ± 2.80 | 2.93 |
| methylophiopogonanone A | 0.5 | 1 | 7.61 | 13.34 | 0.08 | 86.67 ± 7.55 | 8.72 | 81.67 ± 6.98 | 8.54 |
| | | 2 | 6.70 | | | 91.00 ± 10.49 | 11.53 | 89.67 ± 8.52 | 9.51 |
| | | 3 | 7.25 | | | 86.67 ± 8.26 | 9.53 | 96.33 ± 9.75 | 10.12 |
| | 32 | 1 | 6.18 | 6.76 | −0.01 | 94.96 ± 6.68 | 7.03 | 94.50 ± 4.35 | 4.61 |
| | | 2 | 5.09 | | | 88.33 ± 5.82 | 6.59 | 86.51 ± 4.24 | 4.91 |
| | | 3 | 7.71 | | | 91.53 ± 6.00 | 6.55 | 89.39 ± 7.19 | 8.04 |
| | 640 | 1 | 2.14 | 3.08 | −0.01 | 97.44 ± 5.88 | 6.03 | 93.56 ± 5.17 | 5.52 |
| | | 2 | 3.83 | | | 94.51 ± 5.30 | 5.61 | 93.30 ± 5.36 | 5.75 |
| | | 3 | 3.48 | | | 92.04 ± 5.12 | 5.57 | 91.86 ± 5.70 | 6.20 |
| tetrahydropalmatine | 2 | 1 | 4.74 | 12.72 | 0.02 | 97.08 ± 11.43 | 11.77 | 95.17 ± 10.53 | 11.06 |
| | | 2 | 8.34 | | | 86.83 ± 9.39 | 10.81 | 87.25 ± 5.95 | 6.82 |
| | | 3 | 9.44 | | | 88.17 ± 7.12 | 8.07 | 93.75 ± 6.62 | 7.06 |
| | 640 | 1 | 4.55 | 3.41 | 0.01 | 93.87 ± 4.57 | 4.87 | 92.66 ± 3.33 | 3.60 |
| | | 2 | 3.47 | | | 96.27 ± 3.14 | 3.26 | 93.27 ± 2.61 | 2.80 |
| | | 3 | 3.61 | | | 95.08 ± 3.93 | 4.13 | 95.89 ± 2.76 | 2.88 |
| | 3200 | 1 | 6.15 | 1.75 | 0.01 | 94.40 ± 4.13 | 4.38 | 95.91 ± 4.70 | 4.90 |
| | | 2 | 2.13 | | | 93.25 ± 4.40 | 4.72 | 95.03 ± 5.84 | 6.14 |
| | | 3 | 2.08 | | | 95.78 ± 3.07 | 3.20 | 95.51 ± 2.50 | 2.61 |

(*continued on next page*)

**Appendix D** (*continued*)

| Analyte | Concentration (ng/ml) | Batch | Precision | | Accuracy (RE %) | MF (%) | | Recovery (%) | |
|---|---|---|---|---|---|---|---|---|---|
| | | | Intra-day (RSD%) | Inter-day (RSD%) | | Mean ± SD | RSD | Mean ± SD | RSD |
| puerarin | 0.5 | 1 | 5.35 | 11.72 | 0.14 | 91.00 ± 9.86 | 10.83 | 94.33 ± 12.03 | 12.75 |
| | | 2 | 10.93 | | | 92.33 ± 11.41 | 12.36 | 86.67 ± 7.66 | 8.84 |
| | | 3 | 9.61 | | | 87.67 ± 8.24 | 9.40 | 93.00 ± 10.94 | 11.76 |
| | 32 | 1 | 4.75 | 5.57 | −0.02 | 91.46 ± 5.48 | 6.00 | 91.67 ± 5.94 | 6.48 |
| | | 2 | 6.61 | | | 88.52 ± 5.21 | 5.88 | 94.27 ± 6.31 | 6.69 |
| | | 3 | 6.38 | | | 92.79 ± 6.00 | 6.46 | 96.13 ± 4.13 | 4.30 |
| | 640 | 1 | 4.04 | 3.87 | 0.01 | 90.73 ± 5.57 | 6.14 | 95.23 ± 6.23 | 6.54 |
| | | 2 | 3.12 | | | 88.70 ± 4.33 | 4.88 | 90.89 ± 7.11 | 7.82 |
| | | 3 | 3.33 | | | 93.75 ± 4.14 | 4.42 | 89.50 ± 3.12 | 3.49 |
| nobiletin | 2 | 1 | 4.55 | 14.79 | −0.03 | 95.83 ± 8.26 | 8.62 | 88.33 ± 8.84 | 10.01 |
| | | 2 | 7.74 | | | 89.58 ± 5.44 | 6.07 | 96.17 ± 8.76 | 9.11 |
| | | 3 | 7.15 | | | 90.75 ± 8.82 | 9.72 | 95.67 ± 4.64 | 4.85 |
| | 640 | 1 | 2.90 | 3.40 | 0.01 | 94.18 ± 3.65 | 3.87 | 93.15 ± 4.14 | 4.44 |
| | | 2 | 3.43 | | | 92.67 ± 3.16 | 3.41 | 94.30 ± 5.14 | 5.45 |
| | | 3 | 4.85 | | | 94.43 ± 3.43 | 3.63 | 95.70 ± 2.70 | 2.83 |
| | 3200 | 1 | 4.72 | 3.00 | −0.01 | 93.97 ± 4.88 | 5.19 | 94.22 ± 3.13 | 3.32 |
| | | 2 | 1.61 | | | 95.92 ± 4.88 | 5.09 | 95.35 ± 4.04 | 4.24 |
| | | 3 | 2.24 | | | 95.82 ± 4.79 | 5.00 | 94.99 ± 3.61 | 3.80 |
| dehydropachymic acid | 2 | 1 | 5.73 | 12.78 | 0.01 | 96.33 ± 6.43 | 6.68 | 91.17 ± 7.73 | 8.48 |
| | | 2 | 4.95 | | | 92.08 ± 3.29 | 3.58 | 95.50 ± 7.76 | 8.12 |
| | | 3 | 9.25 | | | 93.58 ± 8.22 | 8.79 | 92.42 ± 9.18 | 9.94 |
| | 640 | 1 | 1.71 | 3.46 | −0.01 | 93.32 ± 5.41 | 5.80 | 96.43 ± 2.36 | 2.44 |
| | | 2 | 4.12 | | | 94.34 ± 3.34 | 3.55 | 94.36 ± 3.75 | 3.97 |
| | | 3 | 3.15 | | | 95.92 ± 3.59 | 3.75 | 96.20 ± 3.47 | 3.60 |
| | 3200 | 1 | 3.42 | 2.48 | −0.01 | 96.90 ± 3.98 | 4.11 | 94.92 ± 3.90 | 4.11 |
| | | 2 | 1.46 | | | 93.64 ± 2.43 | 2.60 | 96.01 ± 4.80 | 5.00 |
| | | 3 | 2.11 | | | 93.86 ± 5.21 | 5.55 | 94.10 ± 3.81 | 4.05 |
| cinnamic acid | 1 | 1 | 3.70 | 13.91 | 0.18 | 95.83 ± 5.91 | 6.17 | 89.50 ± 10.84 | 12.11 |
| | | 2 | 6.76 | | | 89.33 ± 9.95 | 11.14 | 87.33 ± 7.42 | 8.50 |
| | | 3 | 6.86 | | | 86.83 ± 8.80 | 10.13 | 86.17 ± 5.49 | 6.37 |
| | 256 | 1 | 1.56 | 3.11 | 0.01 | 89.38 ± 7.74 | 8.66 | 94.95 ± 5.65 | 5.95 |
| | | 2 | 4.94 | | | 90.81 ± 8.34 | 9.19 | 86.96 ± 7.95 | 9.14 |
| | | 3 | 3.89 | | | 90.39 ± 7.96 | 8.81 | 91.81 ± 6.87 | 7.48 |

(*continued on next page*)

**Appendix D** (*continued*)

| Analyte | Concentration (ng/ml) | Batch | Precision | | Accuracy (RE %) | MF (%) | | Recovery (%) | |
|---|---|---|---|---|---|---|---|---|---|
| | | | Intra-day (RSD%) | Inter-day (RSD%) | | Mean ± SD | RSD | Mean ± SD | RSD |
| | 1024 | 1 | 5.92 | 6.08 | 0.06 | 97.35 ± 3.47 | 3.56 | 94.28 ± 6.27 | 6.65 |
| | | 2 | 6.47 | | | 97.07 ± 5.53 | 5.69 | 96.21 ± 5.41 | 5.62 |
| | | 3 | 6.15 | | | 95.96 ± 6.21 | 6.47 | 96.94 ± 4.41 | 4.55 |

QC samples (low, medium, and high concentration levels) were divided into three batches, respectively, and each batch was injected for 6 times on the same day to determine intra-day precision. For three consecutive days, the inter-day precision was calculated, and the accuracy was evaluated by the ratio of the measured value to the true value. The extraction recovery rate was determined by comparing the mean peak area ratios of the analytes in the plasma sample (post-treatment) dissolved in the pre-treatment plasma samples. The matrix effects were detected by comparing the mean peak areas of the analytes dissolved in the pre-treatment plasma sample with that of pure standard solution containing equivalent amounts of the analytes. RSD = SD/X · 100 %, RE = (measured value - actual value)/actual value · 100 %

**Appendix E**

Stability of the 9 analytes in plasma samples under different storage conditions (n = 6)

| Analyte | Concentration (ng/ml) | 24 h at 23 ± 2 °C | | Freeze - thaw 3 times | | −80 °C for 15 days | | Autosampler left for 24 h | |
|---|---|---|---|---|---|---|---|---|---|
| | | Actual concentration | RSD (%) | Actual concentration | RSD (%) | Actual concentration | RSD (%) | Actual concentration | RSD (%) |
| berberine | 0.5 | 0.47 ± 0.02 | 4.36 | 0.61 ± 0.05 | 7.74 | 0.56 ± 0.06 | 10.55 | 0.45 ± 0.05 | 10.94 |
| | 32 | 31.02 ± 1.85 | 5.96 | 31.32 ± 2.21 | 7.06 | 30.24 ± 1.86 | 6.14 | 30.71 ± 1.60 | 5.22 |
| | 640 | 637.90 ± 19.95 | 3.13 | 643.10 ± 14.40 | 2.24 | 623.81 ± 13.14 | 2.11 | 638.56 ± 12.43 | 1.95 |
| trigonelline | 1 | 0.99 ± 0.05 | 4.74 | 0.96 ± 0.09 | 9.66 | 1.06 ± 0.06 | 5.95 | 0.98 ± 0.08 | 8.46 |
| | 256 | 248.16 ± 7.62 | 3.07 | 252.67 ± 6.71 | 2.66 | 255.62 ± 5.98 | 2.34 | 247.84 ± 3.38 | 1.36 |
| | 1024 | 1057.70 ± 36.22 | 3.42 | 1050.32 ± 34.72 | 3.31 | 1037.78 ± 37.60 | 3.62 | 1042.44 ± 12.93 | 1.24 |
| liquiritin | 0.5 | 0.52 ± 0.05 | 9.41 | 0.56 ± 0.06 | 10.98 | 0.56 ± 0.03 | 5.21 | 0.60 ± 0.04 | 6.36 |
| | 32 | 31.20 ± 1.65 | 5.29 | 30.53 ± 1.60 | 5.26 | 31.90 ± 2.07 | 6.50 | 30.53 ± 1.85 | 6.05 |
| | 640 | 626.53 ± 15.98 | 2.55 | 630.75 ± 21.80 | 3.46 | 636.32 ± 22.54 | 3.54 | 632.87 ± 15.18 | 2.40 |
| methylophiopogonanone A | 0.5 | 0.50 ± 0.04 | 8.86 | 0.51 ± 0.04 | 7.66 | 0.51 ± 0.04 | 7.76 | 0.48 ± 0.04 | 9.39 |
| | 32 | 32.12 ± 1.65 | 5.13 | 31.16 ± 1.17 | 3.76 | 32.25 ± 0.98 | 3.03 | 32.61 ± 1.12 | 3.44 |
| | 640 | 623.38 ± 11.17 | 1.79 | 633.87 ± 17.84 | 2.81 | 634.01 ± 16.35 | 2.58 | 631.84 ± 13.28 | 2.10 |
| tetrahydropalmatine | 2 | 2.00 ± 0.11 | 5.45 | 1.99 ± 0.13 | 6.53 | 1.98 ± 0.10 | 5.03 | 2.01 ± 0.11 | 5.45 |
| | 640 | 643.58 ± 11.62 | 1.81 | 637.76 ± 15.85 | 2.49 | 631.85 ± 11.91 | 1.88 | 639.43 ± 13.53 | 2.17 |
| | 3200 | 3180.40 ± 51.40 | 162 | 3196.72 ± 40.92 | 1.28 | 3208.82 ± 59.09 | 1.84 | 3172.33 ± 25.43 | 0.80 |
| puerarin | 0.5 | 0.52 ± 0.04 | 6.95 | 0.44 ± 0.04 | 9.43 | 0.52 ± 0.05 | 9.57 | 0.59 ± 0.06 | 9.41 |
| | 32 | 32.63 ± 1.14 | 3.51 | 31.83 ± 1.26 | 3.95 | 31.81 ± 1.19 | 3.73 | 31.64 ± 1.86 | 5.87 |
| | 640 | 634.07 ± 23.85 | 3.76 | 631.84 ± 13.28 | 2.10 | 631.04 ± 13.50 | 2.14 | 645.89 ± 15.45 | 2.39 |
| nobiletin | 2 | 1.96 ± 0.15 | 7.85 | 2.00 ± 0.11 | 5.72 | 2.03 ± 0.11 | 5.30 | 2.05 ± 0.08 | 3.90 |
| | 640 | 642.90 ± 11.87 | 1.85 | 637.72 ± 11.29 | 1.77 | 646.32 ± 8.26 | 1.28 | 640.76 ± 9.69 | 1.51 |
| | 3200 | 3185.86 ± 56.77 | 1.78 | 3226.79 ± 66.22 | 2.05 | 3175.79 ± 42.07 | 1.32 | 3196.57 ± 57.67 | 1.80 |
| dehydropachymic acid | 2 | 2.01 ± 0.12 | 5.97 | 2.08 ± 0.10 | 4.92 | 2.12 ± 0.07 | 3.28 | 1.92 ± 0.08 | 3.98 |
| | 640 | 639.61 ± 8.64 | 1.35 | 639.72 ± 9.32 | 1.46 | 642.95 ± 10.93 | 1.70 | 634.99 ± 8.69 | 1.37 |
| | 3200 | 3192.25 ± 59.19 | 1.85 | 3232.41 ± 17.03 | 0.53 | 3191.53 ± 60.45 | 1.89 | 3212.86 ± 37.88 | 1.18 |
| cinnamic acid | 1 | 1.04 ± 0.08 | 7.69 | 0.98 ± 0.10 | 9.94 | 0.96 ± 0.08 | 8.74 | 1.06 ± 0.09 | 8.15 |
| | 256 | 356.36 ± 13.40 | 5.23 | 249.31 ± 13.20 | 5.29 | 253.69 ± 12.35 | 4.87 | 253.87 ± 5.72 | 2.25 |
| | 1024 | 1014.61 ± 47.42 | 4.67 | 1005.37 ± 40.84 | 4.06 | 1033.73 ± 47.90 | 4.63 | 1007.69 ± 62.85 | 6.24 |

QC samples (low, medium, and high concentration levels) were exposed to 24 h at 23 ± 2 °C, freeze - thaw 3 times, −80 °C for 15 days, and autosampler left for 24 h, calculated the RSD to determine the stability.

## References


[1] T. De Coster, P. Claus, I.V. Kazbanov, P. Haemers, R. Willems, K.R. Sipido, A.V. Panfilov, Arrhythmogenicity of fibro-fatty infiltrations, Sci. Rep. 8 (1) (2018) 2050, https://doi.org/10.1038/s41598-018-20450-w.

[2] S. Nattel, D. Dobrev, Electrophysiological and molecular mechanisms of paroxysmal atrial fibrillation, Nat. Rev. Cardiol. 13 (10) (2016) 575–590, https://doi.org/10.1038/nrcardio.2016.118.

[3] J.N. Weiss, A. Garfinkel, H.S. Karagueuzian, T.P. Nguyen, R. Olcese, P.S. Chen, Z. Qu, Perspective: a dynamics-based classification of ventricular arrhythmias, J. Mol. Cell. Cardiol. 82 (2015) 136–152, https://doi.org/10.1016/j.yjmcc.2015.02.017.

[4] L. Xiao, Y. Ma, F. Sun, F. Yang, L. Zhang, C. Zhang, J. Hu, B. Zhang, H. Shang, G. Li, New progress in the treatment of arrhythmia: TCM integrated regulation, Zhonghua Journal of Traditional Chinese Medicine 30 (11) (2015) 3856–3860.

[5] J. Chen, Z. Liu, F. Deng, J. Liang, B. Fan, X. Zhen, R. Tao, L. Sun, S. Zhang, Z. Cong, X. Li, W. Du, Mechanisms of Lian-Gui-Ning-Xin-Tang in the treatment of arrhythmia: integrated pharmacology and in vivo pharmacological assessment, Phytomedicine 99 (2022) 153989, https://doi.org/10.1016/j.phymed.2022.153989.

[6] X. Li, J. Liu, F. Deng, J. Chen, B. Fan, J. Liang, W. Du, Differentiation and treatment of arrhythmia from Qihua theory, Liaoning Journal of Traditional Chinese Medicine 49 (7) (2022) 64–66, https://doi.org/10.13192/j.issn.1000-1719.2022.07.019.

[7] J. Liang, J. Chen, F. Deng, B. Fan, W. Du, Treating tachyarrhythmia under guidance of "one Qi circulation" theory, Liaoning Journal of Traditional Chinese Medicine 49 (6) (2022) 61–63, https://doi.org/10.13192/j.issn.1000-1719.2022.06.016.

[8] A. Salama, R.E. Mostafa, E.A. Omara, Effects of phosphodiestrase type 5 inhibitors in epinephrine-induced arrhythmia in rats: Involvement of lactate dehydrogenase and creatine kinase downregulation and adiponectin expression, Hum. Exp. Toxicol. 37 (3) (2018) 256–264, https://doi.org/10.1177/0960327117695638.

[9] M.J. Curtis, J.C. Hancox, A. Farkas, C.L. Wainwright, C.L. Stables, D.A. Saint, J.H. Clements, P.D. Lambiase, G.E. Billman, M.J. Janse, M.K. Pugsley, G.A. Ng, D. M. Roden, A.J. Camm, M.J.A. Walker, The Lambeth conventions (II): guidelines for the study of animal and human ventricular and supraventricular arrhythmias, Pharmacol. Ther. 139 (2) (2013) 231–248, https://doi.org/10.1016/j.pharmthera.2013.04.008.

[10] F. De Clerck, A. Van de Water, J. D'Aubioul, H.R. Lu, K. van Rossem, A. Hermans, K. Van Ammel, In vivo measurement of QT prolongation, dispersion and arrhythmogenesis: application to the preclinical cardiovascular safety pharmacology of a new chemical entity, Fundam. Clin. Pharmacol. 16 (2) (2002) 125–140, https://doi.org/10.1046/j.1472-8206.2002.00081.x.

[11] J.H. van Berlo, M. Maillet, J.D. Molkentin, Signaling effectors underlying pathologic growth and remodeling of the heart, J. Clin. Invest. 123 (1) (2013) 37–45, https://doi.org/10.1172/JCI62839.

[12] J. Wang, W. Dong, B. Jiang, D. Li, W. Zhang, J. Wang, Y. Mu, Y. Li, Y. Chen, Effect of icariin on ventricular arrhythmia induced by congestive heart failure in rabbits and its electrophysiological mechanism, Chinese Journal of Medical Physics 37 (2020) 361–367, https://doi.org/10.3969/j.issn.1005-202X.2020.03.020.

[13] K. Pytka, K. Lustyk, E. Żmudzka, M. Kotańska, A. Siwek, M. Zygmunt, A. Dziedziczak, J. Śniecikowska, A. Olczyk, A. Gałuszka, J. Śmieja, A.M. Waszkielewicz, H. Marona, B. Filipek, J. Sapa, S. Mogilski, Chemically Homogenous compounds with antagonistic properties at all α1-Adrenoceptor subtypes but not β1-Adrenoceptor Attenuate adrenaline-induced arrhythmia in rats, Front. Pharmacol. 7 (2016) 229, https://doi.org/10.3389/fphar.2016.00229.

[14] P. Türck, A. Nemec-Bakk, T. Talwar, Z. Suntres, A. Belló-Klein, A.S. da Rosa Araujo, N. Khaper, Blueberry extract attenuates norepinephrine-induced oxidative stress and apoptosis in H9c2 cardiac cells, Mol. Cell. Biochem. 477 (3) (2022) 663–672, https://doi.org/10.1007/s11010-021-04313-z.

[15] A. Adameova, A.K. Shah, N.S. Dhalla, Role of oxidative stress in the Genesis of ventricular arrhythmias, Int. J. Mol. Sci. 21 (12) (2020) 4200, https://doi.org/10.3390/ijms21124200.

[16] M. Radaković, S. Borozan, N. Djelić, S. Ivanović, D.Ć. Miladinović, M. Ristanić, B. Spremo-Potparević, Z. Stanimirović, Nitroso-oxidative stress, acute phase response, and Cytogenetic damage in Wistar rats treated with adrenaline, Oxid. Med. Cell. Longev. (2018) 1805354, https://doi.org/10.1155/2018/1805354.

[17] Y. Yin, W. Han, Y. Cao, Association between activities of SOD, MDA and Na+-K+-ATPase in peripheral blood of patients with acute myocardial infarction and the complication of varying degrees of arrhythmia, Hellenic J. Cardiol. 60 (6) (2019) 366–371, https://doi.org/10.1016/j.hjc.2018.04.003.

[18] H. El Hadi, R. Vettor, M. Rossato, Cardiomyocyte mitochondrial dysfunction in diabetes and its contribution in cardiac arrhythmogenesis, Mitochondrion 46 (2019) 6–14, https://doi.org/10.1016/j.mito.2019.03.005.

[19] J.X. Nicoll, A.C. Fry, E.M. Mosier, The effects of a caffeine containing pre-workout supplement on β2-adrenergic and MAPK signaling during resistance exercise, Eur. J. Appl. Physiol. 123 (3) (2023) 585–599, https://doi.org/10.1007/s00421-022-05085-0.

[20] A. Maimaitiaili, J. Li, A. Aibibula, M. Abudureheman, Inhibition of nuclear factor kappa B pathway protects myocardial ischemia/reperfusion injury in rats under treatment with abnormal savda munziq, Am J Transl Res 10 (1) (2018) 77–85.

[21] B. Bai, Y. Yang, Q. Wang, M. Li, C. Tian, Y. Liu, L.H.H. Aung, P.F. Li, T. Yu, X.M. Chu, NLRP3 inflammasome in endothelial dysfunction, Cell Death Dis. 11 (9) (2020) 776, https://doi.org/10.1038/s41419-020-02985-x.

[22] A.P. Landstrom, D. Dobrev, X.H.T. Wehrens, Calcium signaling and cardiac arrhythmias, Circ. Res. 120 (12) (2017) 1969–1993, 10.1161/CIRCRESAHA.117.310083.

[23] X. Liu, W. Zhang, J. Luo, W. Shi, X. Zhang, Z. Li, X. Qin, B. Liu, Y. Wei, TRIM21 deficiency protects against atrial inflammation and remodeling post myocardial infarction by attenuating oxidative stress, Redox Biol. 62 (2023) 102679, https://doi.org/10.1016/j.redox.2023.102679.

[24] L. Zu, N. Wen, C. Liu, M. Zhao, L. Zheng, Connexin43 and myocardial ischemia-reperfusion injury, Cardiovasc. Hematol. Disord.: Drug Targets 18 (1) (2018) 14–16, https://doi.org/10.2174/1871529X16666161227143644.

[25] L. Leybaert, M.A. De Smet, A. Lissoni, R. Allewaert, H.L. Roderick, G. Bultynck, M. Delmar, K.R. Sipido, K. Witschas, Connexin hemichannels as candidate targets for cardioprotective and anti-arrhythmic treatments, J. Clin. Invest. 133 (6) (2023) e168117, https://doi.org/10.1172/JCI168117.

[26] T. Wang, J. Liu, C. Hu, X. Wei, L. Han, A. Zhu, R. Wang, Z. Chen, Z. Xia, S. Yao, W. Mao, Downregulation of cardiac PIASy inhibits Cx43 SUMOylation and ameliorates ventricular arrhythmias in a rat model of myocardial ischemia/reperfusion injury, Chin Med J (Engl). 136 (11) (2023) 1349–1357, https://doi.org/10.1097/CM9.0000000000002618.

[27] C. Bueno-Beti, C.X. Lim, A. Protonotarios, P.L. Szabo, J. Westaby, M. Mazic, M.N. Sheppard, E. Behr, O. Hamza, A. Kiss, B.K. Podesser, M. Hengstschläger, T. Weichhart, A. Asimaki, An mTORC1-dependent mouse model for cardiac Sarcoidosis, J. Am. Heart Assoc. 12 (19) (2023) e030478, https://doi.org/10.1161/JAHA.123.030478.

[28] M.A. Lillo, M. Muñoz, P. Rhana, K. Gaul-Muller, J. Quan, N. Shirokova, L.H. Xie, L.F. Santana, D. Fraidenraich, J.E. Contreras, Remodeled connexin 43 hemichannels alter cardiac excitability and promote arrhythmias, J. Gen. Physiol. 155 (7) (2023) e202213150, https://doi.org/10.1085/jgp.202213150.

[29] J.L. Solan, P.D. Lampe, Spatio-temporal regulation of connexin43 phosphorylation and gap junction dynamics, Biochim. Biophys. Acta Biomembr. 1860 (1) (2018) 83–90, https://doi.org/10.1016/j.bbamem.2017.04.008.

[30] C.J. van Opbergen, M. Delmar, T.A. van Veen, Potential new mechanisms of pro-arrhythmia in arrhythmogenic cardiomyopathy: focus on calcium sensitive pathways, Neth. Heart J. 25 (3) (2017) 157–169, https://doi.org/10.1007/s12471-017-0946-7.

[31] T. Chen, B. Kong, W. Shuai, Y. Gong, J. Zhang, H. Huang, Vericiguat alleviates ventricular remodeling and arrhythmias in mouse models of myocardial infarction via CaMKII signaling, Life Sci. 334 (2023) 122184, https://doi.org/10.1016/j.lfs.2023.122184.

[32] L. Cao, Y. Chen, L. Lu, Y. Liu, Y. Wang, J. Fan, Y. Yin, Angiotensin II upregulates fibroblast-myofibroblast transition through Cx43-dependent CaMKII and TGF-β1 signaling in neonatal rat cardiac fibroblasts, Acta Biochim. Biophys. Sin. 50 (9) (2018) 843–852, https://doi.org/10.1093/abbs/gmy090.

[33] A. Hammerer-Lercher, M. Namdar, N. Vuilleumier, Emerging biomarkers for cardiac arrhythmias, Clin. Biochem. 75 (2020) 1–6, https://doi.org/10.1016/j.clinbiochem.2019.11.012.

[34] F.E. Fakuade, V. Steckmeister, F. Seibertz, J. Gronwald, S. Kestel, J. Menzel, J.R.D. Pronto, K. Taha, F. Haghighi, G. Kensah, C.M. Pearman, F. Wiedmann, A. J. Teske, C. Schmidt, K.M. Dibb, A. El-Essawi, B.C. Danner, H. Baraki, B. Schwappach, I. Kutschka, F.E. Mason, N. Voigt, Altered atrial cytosolic calcium handling contributes to the development of postoperative atrial fibrillation, Cardiovasc. Res. 117 (7) (2021) 1790–1801, https://doi.org/10.1093/cvr/cvaa162.

[35] V. Paar, P. Jirak, R. Larbig, N.S. Zagidullin, M.C. Brandt, M. Lichtenauer, U.C. Hoppe, L.J. Motloch, Pathophysiology of calcium mediated ventricular arrhythmias and novel therapeutic Options with focus on Gene Therapy, Int. J. Mol. Sci. 20 (21) (2019) 5304, https://doi.org/10.3390/ijms20215304.
[36] C.H. Yeh, Z.Q. Shen, S.Y. Hsiung, P.C. Wu, Y.C. Teng, Y.J. Chou, S.W. Fang, C.F. Chen, Y.T. Yan, L.S. Kao, C.H. Kao, T.F. Tsai, Cisd2 is essential to delaying cardiac aging and to maintaining heart functions, PLoS Biol. 17 (10) (2019) e3000508, 10.1371/journal.pbio.3000508.
[37] J. Skogestad, J.M. Aronsen, N. Tovsrud, P. Wanichawan, K. Hougen, M.K. Stokke, C.R. Carlson, I. Sjaastad, O.M. Sejersted, F. Swift, Coupling of the $Na^+/K^+$-ATPase to Ankyrin B controls $Na^+/Ca^{2+}$ exchanger activity in cardiomyocytes, Cardiovasc. Res. 116 (1) (2020) 78–90, https://doi.org/10.1093/cvr/cvz087.
[38] Y. Zhao, X. Wang, C. Chen, K. Shi, J. Li, R. Du, Protective effects of 3,4-Seco-Lupane Triterpenes from Food Raw materials of the Leaves of Eleutherococcus Senticosus and Eleutherococcus Sessiliflorus on arrhythmia induced by barium Chloride, Chem. Biodivers. 18 (4) (2021) e2001021, https://doi.org/10.1002/cbdv.202001021.
[39] H. Altay, Y. Çavuşoğlu, A. Çelik, Ş. Demir, B. Kılıçarslan, S. Nalbantgil, A. Temizhan, B. Tokgöz, D. Ural, D. Yeşilbursa, Ö. Yıldırımtürk, M.B. Yılmaz, Management of hyperkalemia in heart failure, Turk Kardiyol Dern Ars 49 (Supp1) (2021) 1–32, https://doi.org/10.5543/tkda.2021.S1.
[40] G.L. Kearns, M. Artman, Functional biomarkers: an approach to Bridge pharmacokinetics and pharmacodynamics in Pediatric clinical Trials, Curr Pharm Des 21 (39) (2015) 5636–5642, https://doi.org/10.2174/1381612821666150901105337.
[41] M. Lv, D. Yang, X. Ji, L. Lou, B. Nie, J. Zhao, A. Wu, M. Zhao, Effect of WenXin KeLi on Improvement of arrhythmia after myocardial infarction by intervening PI3K-AKT-mTOR Autophagy pathway, Evid Based Complement Alternat Med (2022) 2022970, https://doi.org/10.1155/2022/2022970.
[42] R. Guo, L. Li, J. Su, S. Li, S.E. Duncan, Z. Liu, G. Fan, Pharmacological activity and mechanism of Tanshinone IIA in related diseases, Drug Des Devel Ther 14 (2020) 4735–4748, https://doi.org/10.2147/DDDT.S266911.
[43] X. Han, X. Liu, X. Zhao, X. Wang, Y. Sun, C. Qu, J. Liang, B. Yang, Dapagliflozin ameliorates sepsis-induced heart injury by inhibiting cardiomyocyte apoptosis and electrical remodeling through the PI3K/Akt pathway, Eur. J. Pharmacol. 955 (2023) 175930, https://doi.org/10.1016/j.ejphar.2023.175930.
[44] Y. Li, Q. Li, C. Wang, Z. Lou, Q. Li, Trigonelline reduced diabetic nephropathy and insulin resistance in type 2 diabetic rats through peroxisome proliferator-activated receptor-γ, Exp. Ther. Med. 18 (2) (2019) 1331–1337, https://doi.org/10.3892/etm.2019.7698.
[45] Q. Zhou, Y. Zhang, B. Wang, W. Zhou, Y. Bi, W. Huai, X. Chen, Y. Chen, Z. Liu, X. Liu, Z. Zhan, KDM2B promotes IL-6 production and inflammatory responses through Brg1-mediated chromatin remodeling, Cell. Mol. Immunol. 17 (8) (2020) 834–842, https://doi.org/10.1038/s41423-019-0251-z.
[46] A.G. Kléber, Q. Jin, Coupling between cardiac cells-An important determinant of electrical impulse propagation and arrhythmogenesis, Biophys Rev (Melville) 2 (3) (2021) 031301, https://doi.org/10.1063/5.0050192.
[47] I. Epifantseva, R.M. Shaw, Intracellular trafficking pathways of Cx43 gap junction channels, Biochim. Biophys. Acta Biomembr. 1860 (1) (2018) 40–47, https://doi.org/10.1016/j.bbamem.2017.05.018.
[48] Z. Li, D. Liu, X. Wang, J. Zhuang, Application prospect of trigonelline in regulating metabolic disorders after renal transplantation, Organ Transplantation 12 (2021) 363–368, https://doi.org/10.3969/j.issn.1674-7445.2021.03.017.
[49] J. Zhao, L. Yu, X. Xue, Y. Xu, T. Huang, D. Xu, Z. Wang, L. Luo, H. Wang, Diminished α7 nicotinic acetylcholine receptor (α7nAChR) rescues amyloid-β induced atrial remodeling by oxi-CaMKII/MAPK/AP-1 axis-mediated mitochondrial oxidative stress, Redox Biol. 59 (2023) 102594, https://doi.org/10.1016/j.redox.2022.102594.